Diversity of ancestral brainstem noradrenergic neurons across species and multiple biological factors

Michael A. Kelberman[1, 2, *], Ellen Rodberg[3, 4, *], Ehsan Arabzadeh[5], Chloe J. Bair-Marshall[6], Craig W. Berridge[7], Esther Berrocoso[8, 9], Vincent Breton-Provencher[10], Daniel J. Chandler[11], Alicia Che[12, 13], Oscar Davy[14], David M. Devilbiss[11], Anthony M. Downs[15, 16], Gabrielle Drummond[17], Roman Dvorkin[18], Zeinab Fazlali[19, 20, 21], Robert C. Froemke[6, 22], Erin Glennon[6, 23], Joshua I. Gold[24], Hiroki Ito[14, 25], Xiaolong Jiang[26, 27], Joshua P. Johansen[28], Alfred P. Kaye[12, 13, 29], Jenny R. Kim[30], Chao-Cheng Kuo[30, 34], Rong-Jian Liu[12], Yang Liu[31], Meritxell Llorca-Torralba[8, 9], Jordan G. McCall[30], Zoe A. McElligott[15, 16, 32], Andrew M. McKinney[26], Cristina Miguelez[33], Ming-Yuan Min[34], Alexandra C. Nowlan[15], Mohsen Omrani[35], Gina R. Poe[36], Anthony Edward Pickering[14], Yadollah Ranjbar-Slamloo[19], Jone Razquin[33], Charles Rodenkirch[31], Anna C. Sales[14], Rath Satyasambit[28, 37], Stephen D. Shea[18], Mriganka Sur[17], John Arthur Tkaczynski[11], Sonia Torres-Sanchez[8, 9], Akira Uematsu[38], Chayla R. Vazquez[30], Amelien Vreven[39, 40, 41], Qi Wang[31], Barry D Waterhouse[11], Hsiu-Wen Yang[42], Jen-Hau Yang[12, 43], Liping Zhao[44], Ioannis S. Zouridis[45, 46], David Weinshenker[2], Elena Vazey[3, 4], Nelson K. Totah[39, 40, 41, 46, C]

*Denotes equal contribution; authors ordered alphabetically by last name

[C] Corresponding author contact: nelson.totah@helsinki.fi

[1]Department of Molecular, Cellular and Developmental Biology, University of Colorado Boulder, Boulder, CO, USA

[2]Department of Human Genetics, Emory University, Atlanta, GA, USA

[3]Department of Biology, University of Massachusetts Amherst, Amherst, MA, USA

[4]Neuroscience and Behavior Program, University of Massachusetts Amherst, Amherst, MA, USA

[5]Eccles Institute of Neuroscience, John Curtin School of Medical Research, The Australian National University, Canberra, AUS

[6]Neuroscience Institute, NYU Langone Medical Center, New York University, New York, New York, USA

[7]Department of Psychology, University of Wisconsin-Madison, Madison, WI, USA

[8]Neuropsychopharmacology and Psychobiology Research Group, Department of Neuroscience, School of Medicine, Biomedical Research and Innovation Institute of Cádiz (INiBICA), University of Cadiz, Cadiz, Spain

[9]Centro de Investigación Biomédica en Red de Salud Mental (CIBERSAM), Instituto de Salud Carlos III, Madrid, Spain

[10]Department of Psychiatry and Neuroscience, Université Laval, Québec, QC, Canada

[11]Department of Neuroscience, Rowan-Virtua SOM, Stratford, NJ, USA

[12]Department of Psychiatry, Yale University School of Medicine, New Haven, CT, USA

[13]Wu Tsai Institute, Yale University, New Haven, CT, USA

[14]School of Physiology, Pharmacology and Neuroscience, University of Bristol, Bristol, United Kingdom

[15]Bowles Center for Alcohol Studies, University of North Carolina at Chapel Hill, Chapel Hill, NC, USA

[16]Department of Pharmacology, University of North Carolina at Chapel Hill, Chapel Hill, NC, USA

[17]Department of Brain and Cognitive Sciences, Picower Institute for Learning and Memory, Massachusetts Institute of Technology, Cambridge, MA, USA

[18]Cold Spring Harbor Laboratory, Cold Spring Harbor, NY, USA

[19]School of Cognitive Sciences, Institute for Research in Fundamental Sciences (IPM), Tehran, Iran

[20]Department of Psychiatry, Columbia University, New York, NY, USA
[21]New York State Psychiatric Institute, New York, NY, USA
[22]Department of Otolaryngology, NYU Grossman School of Medicine, New York, NY, USA
[23]Department of Neurology, Weill Cornell Medicine, New York
[24]Department of Neuroscience, University of Pennsylvania, Philadelphia, PA, USA
[25]Department of Urology, Yokohama City University Graduate School of Medicine, Yokohama, Japan
[26]Department of Neuroscience, Baylor College of Medicine Neurological Research Institute at Texas Children's Hospital, 1250, Houston, TX, USA
[27]Department of Ophthalmology, Baylor College of Medicine Neurological Research Institute at Texas Children's Hospital, 1250, Houston, TX, USA
[28]RIKEN Center for Brain Science, Wako-shi Saitama, Japan
[29]Clinical Neurosciences Division, VA National Center for PTSD, West Haven, CT, USA
[30]Department of Anesthesiology, Washington University in St. Louis, St. Louis, MO, USA
[31]Department of Biomedical Engineering, Columbia University, New York, NY, USA
[32]Department of Psychiatry, University of North Carolina at Chapel Hill, Chapel Hill, NC, USA
[33]Department of Pharmacology, Faculty of Medicine and Nursing, University of the Basque Country (UPV/EHU), Leioa, Bizkaia, Spain
[34]Department of Life Science, College of Life Science, National Taiwan University, Taipei, Taiwan
[35]Department of Psychiatry, Queen's University, Kingston, ON, Canada
[36]Integrative Biology and Physiology, UCLA, Los Angeles, CA, USA
[37]Department of Computer Science, Tokyo Institute of Technology, Midori, Yokohama, Japan
[38]Human Informatics and Information Research Institute, National Institute of Advanced Industrial Science and Technology, Japan
[39]Helsinki Institute of Life Science (HiLIFE), University of Helsinki, Helsinki, Finland
[40]Neuroscience Center, University of Helsinki, Helsinki, Finland
[41]Faculty of Pharmacy, University of Helsinki, Helsinki, Finland
[42]Department of Biomedical Sciences, Chung-Shan Medical University, Taichung, Taiwan
[43]Doctoral Program of Clinical and Experimental Medicine, National Sun Yat-sen University, Kaohsiung, Taiwan
[44]Department of Biostatistics and Bioinformatics, Rollins School of Public Health, Emory University, Atlanta, GA USA
[45]Graduate Training Centre of Neuroscience, International Max Planck Research School (IMPRS), University of Tübingen, Tübingen, Germany
[46]Department of Physiology of Cognitive Processes, Max Planck Institute for Biological Cybernetics, Tübingen, Germany

Abstract

The brainstem region, locus coeruleus (LC), has been remarkably conserved across vertebrates. Evolution has woven the LC into wide-ranging neural circuits that influence functions as broad as autonomic systems, the stress response, nociception, sleep, and high-level cognition among others. Given this conservation, there is a strong possibility that LC activity is inherently similar across species, and furthermore that age, sex, and brain state influence LC activity similarly across species. The degree to which LC activity is homogenous across these factors, however, has never been assessed due to the small sample size of individual studies. Here, we pool data from 20 laboratories (1,855 neurons) and show diversity across both intrinsic and extrinsic factors such as species, age, sex and brain state. We use a negative binomial regression model to compare activity from male monkeys, and rats and mice of both sexes that were recorded across brain states from brain slices *ex vivo* or under different anesthetics or during wakefulness *in vivo*. LC activity differed due to complex interactions of species, sex, and brain state. The LC became more active during aging, independent of sex. Finally, in contrast to the foundational principle that all species express two distinct LC firing modes ("tonic" or "phasic"), we discovered great diversity within spontaneous LC firing patterns. Different factors were associated with higher incidence of some firing modes. We conclude that the activity of the evolutionarily-ancient LC is not conserved. Inherent differences due to age and species-sex-brain state interactions have implications for understanding the role of LC in species-specific naturalistic behavior, as well as in psychiatric disorders, cardiovascular disease, immunology, and metabolic disorders.

Introduction

The central nervous system-wide projection pattern of the brainstem noradrenergic cell group A6, locus coeruleus (LC), has been retained across the vertebrate phylogenetic tree (Ma, 1994; Smeets and Gonzalez, 2000; Manger and Eschenko, 2021; Wang et al., 2022; Vreven et al., 2024). In addition to retention of LC projection structure, one of the core functions of the LC – mobilization of physiological resources in response to the need for physical energy expenditure and/or cognitive energy expenditure (i.e., arousal or brain state) – has been conserved across vertebrate nervous systems (Aston-Jones and Bloom, 1981a; Bouret and Sara, 2005; Castelino and Schmidt, 2010; Varazzani et al., 2015; Lovett-Barron et al., 2017; Hayat et al., 2020). Therefore, the activity patterns of LC neurons may have also been conserved across vertebrates to fulfill a fundamental functional role. Consider the analogy of breathing, which is fundamentally the same across mammals: it is controlled by identical activity patterns in a

homologous brainstem cell group, the pre-Bötzinger complex (Ramirez et al., 2016; Del Negro et al., 2018). The same may be the case for the LC and its arousal function. Indeed, across multiple species, the *population* mean baseline firing rate of LC neurons is ~ 1 spike/sec under anesthesia, sleep, or wakefulness (Vreven et al., 2024). Furthermore, LC functional firing properties, such as the phasic burst response to salient stimuli or elevated baseline firing in the context of anxiety and the stress response, are conserved across species (Aston-Jones and Bloom, 1981b, a; Hirata and Aston-Jones, 1994; Vankov et al., 1995; Curtis et al., 2012; McCall et al., 2015; Hayat et al., 2020; Prokopiou et al., 2022). Finally, two modes of LC activity (tonic and phasic) have been defined in non-human primates (NHPs) (Foote et al., 1980; Grant et al., 1988; Aston-Jones et al., 1994; Joshi et al., 2016) and rodents alike (Aston-Jones and Bloom, 1981b, a; Akaike, 1982; Harley and Sara, 1992; Vankov et al., 1995; Vazey and Aston-Jones, 2014; Kelberman et al., 2023; Li et al., 2023). This dual-mode of operation is an universal principal in neuroscience. In sum, a large body of evidence supports the hypothesis that LC activity is fundamentally similar across species to fulfill similar functions.

However, this hypothesis has never been tested because individual studies of LC activity are almost always conducted in a single species and have small sample sizes. Intracellular recordings target one neuron and typically pool data across experiments into sample sizes of less than 75 neurons per study (Chandler et al., 2014; McCall et al., 2015; Li et al., 2016; Prouty et al., 2017; Borodovitsyna et al., 2018; Breton-Provencher and Sur, 2019; Kuo et al., 2020; Borodovitsyna et al., 2022; Tkaczynski et al., 2022; Downs et al., 2023; Kuo et al., 2023; McKinney et al., 2023). Extracellular recording can record discharge patterns from many neurons (“single units”) simultaneously; however, in awake (even head-fixed) rodents and non-human primates (NHPs), physical instability of the electrode-tissue interface caused by cardiac, respiratory, and spinal movement reduces recording yield to one or two neurons per experiment (Kalwani et al., 2014; Swift et al., 2018; Breton-Provencher and Sur, 2019). These small sample sizes have prevented the comparison of LC activity across the wide range of species, disease-related animal models, and experimental preparations used in basic and translational neuroscience.

A systematic assessment of how species, sex, age, and experimental preparation affect LC activity is necessary to explain the neural basis of behaviors that are species- or sex-dependent and to understand sex- and age-specific disease prevalence (Brady and Randall, 1999; Whitacre, 2001; Kessler, 2003; Tolin and Foa, 2006; Lovejoy et al., 2009; Appelman et al., 2015; Bangasser et al., 2016; Ferretti et al., 2018; Weinshenker, 2018; Poe et al., 2020). The LC, via its ascending brain-wide projections, is implicated in cognitive deficits observed in attention deficit and hyperactivity disorder, schizophrenia, and

neurodegenerative diseases (Aston-Jones and Cohen, 2005; Sara, 2009; Poe et al., 2020) as well as psychological and physical symptoms of post-traumatic stress disorder, anxiety disorder, and symptoms of opioid withdrawal (Weinshenker and Schroeder, 2007; Weinshenker, 2018; Llorca-Torralba et al., 2019; Morris et al., 2020; Poe et al., 2020; Ross and Van Bockstaele, 2020). Moreover, via descending projections to the autonomic nervous system and the spinal cord, the LC influences peripheral pain analgesia, cardiovascular disease, immune dysfunction, metabolic disorders, and obesity (Abercrombie and Jacobs, 1987; Sved and Felsten, 1987; Ziegler et al., 1999; Almeida et al., 2004; Glaser and Kiecolt-Glaser, 2005; Mawdsley and Rampton, 2005; Nemeroff and Goldschmidt-Clermont, 2012; Tovar et al., 2013; Bravo et al., 2014; Wang et al., 2014; Hirschberg et al., 2017; Osorio-Forero et al., 2021; Berrocoso et al., 2022; Poller et al., 2022; Williams and Rahmouni, 2022; Anderson et al., 2023; Fortin et al., 2023). The relevance of LC to such a broad range of human health and disease conditions underscores the importance of understanding how LC activity varies with respect to species, sex, age, and experimental preparation.

Here, we pooled recordings from 20 laboratories totaling 1,855 verified single units spanning three species, various ages, both sexes, multiple brain states or experimental preparation types, as well as genetic and disease-modelling manipulations. We report that LC firing rate is influenced by age and genetic modifications, and by a complex interaction between species, sex, and brain state and experimental preparation. Intriguingly, most disease models did not show altered firing rate of LC neurons. Moreover, unsupervised k-means clustering of firing patterns uncovered novel spontaneous firing patterns which are differentially expressed depending on species, sex, age, and brain state (defined by type of experimental preparation).

Results

We compiled spontaneously occurring spike trains of LC neurons collected by 20 laboratories. These data included mice and rats of both sexes, as well as male NHPs (the Old World primate, Macaca mulatta). Animals spanned relatively young (adolescent) to adult and late age. Spike discharges were recorded either in tissue slices (intracellular), intact animals under anesthesia of various types, or during wakefulness. Additionally, some LC neurons or animals were genetically modified for optogenetic manipulation and, while recordings during optogenetic stimulation were not included in the data set, the genetic modification was considered as a factor that could influence firing rate. Finally, a subset of mice were pharmacologically manipulated or bred to express disease-specific genotypes.

Laboratories providing extracellular recordings were asked to include only single units (henceforth referred to as "neurons"). However, in the interest of applying similar criteria to define single units across laboratories, we performed a quality control sweep of the 2,944 neurons (**Figure 1**). We discarded neurons for which more than 2% of the interspike intervals were less than 10 msec as described in prior work (Totah et al., 2018). This excluded 319 neurons from further analysis. Next, we removed spiking occurring during pharmacological manipulation with the exception of anesthesia. We sought to characterize only temporally stable recordings and removed neurons which did not spike more than 30 times throughout the recording (457 neurons were removed). At the request of the contributors of those data we also removed 199 neurons that were recorded from animals subjected to a stressor. Additionally, we removed 113 neurons in which the sex of the animal was unknown; this was necessary because the negative binomial regression model required each neuron to have information about each factor that could affect firing rate. These exclusions left only one neuron recorded under pentobarbital anesthesia, which was removed from subsequent analyses. After submitting data to this quality control procedure, a total of 1,855 neurons remained for analysis of firing rates. The number of neurons for each factor are reported in **Table 1**. Finally, since some recordings were provided with stimulus-evoked spiking following a stimulus-free baseline epoch, we determined for each neuron whether there was significant difference in the mean firing rate between the epoch of the recording without stimulation and the subsequent recording epoch containing sensory stimuli. We reasoned that, since phasic LC responses to stimuli are transient biphasic events lasting ~1000 msec (Aston-Jones and Bloom, 1981b), such transient changes would not lead to an overall change in firing rate averaged over a comparably much larger time window (the duration of this subset of recordings ranged from ~5 seconds to ~7 hours, and the median duration was 444 sec). We performed a Student's t-test comparing multiple samples of firing rate (split into 10 equal time bins) between the recording epochs with, or without, sensory stimuli. If the introduction of sensory stimuli led to a significant ($p<0.05$) alteration of time-averaged firing rate compared to the preceding stimulus-free epoch, then the spike train of that neuron was analyzed only until the first stimulus and the remaining data were discarded. Out of 1,855 neurons, 560 were exposed to sensory stimuli; of those 560, we discarded the recording epoch with stimuli for 352 neurons. In addition to analyzing firing rate, we also analyzed firing patterns and, for that analysis, only included spike trains of individual neurons prior to any stimuli. Further, we excluded units that did not have at least 100 interspike intervals (ISIs) prior to any stimulus or pharmacology application but included neurons from animals with an unreported sex to increase sample size (1708 neurons analyzed).

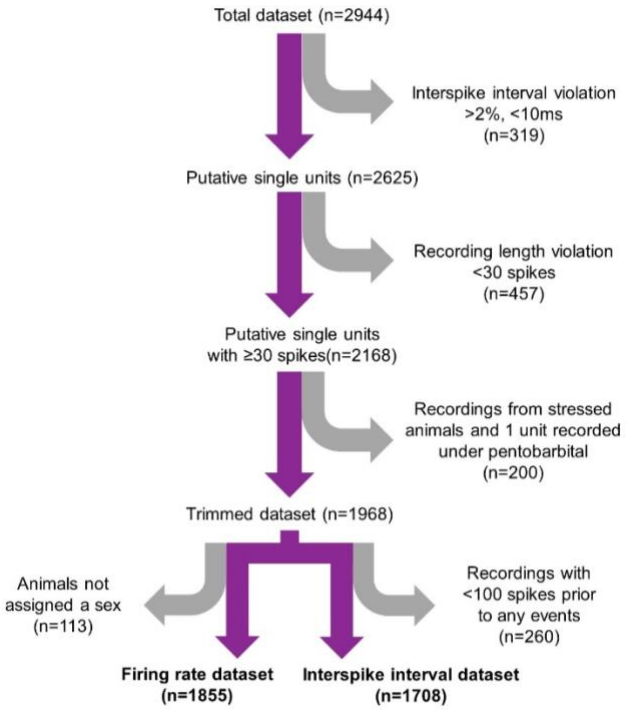

Figure 1. A quality control flowchart showing the steps used to check the quality of the submitted data. A flowchart visualizing the quality control steps of submitted data. Grey arrows indicate removal of neurons from the data set and the number of neurons removed is in parentheses. The number reported below each purple arrow shows the number of remaining neurons subjected to the next step in the quality control process. To maintain the largest appropriate dataset, slightly different criteria were used to qualify neurons be included for firing rate analysis (left, n=1855) vs. interspike interval analysis (right, n=1708).

Table 1: Summary of the characteristics of the dataset after quality control. The percentages are based upon the total number of neurons subjected to analysis of firing rate (n = 1,855). WT refers to wild-type animals that were unmanipulated and not on another genetic background (i.e. cre-lines). Rodents were designated as adolescent (<3 months), adult (3-12 months), or aged (>12 months), while all NHP data came from adult animals (10-16 years) (Dutta and Sengupta, 2016; Simmons, 2016; Colman, 2018; Chiou et al., 2020; Wang et al., 2020; Delage et al., 2021).

Species	Sex	Strain	Genotype/Intervention	Age	State				
					Awake	Anesthesia			Slice (Whole Cell, Cell Attached)
						Isoflurane	Chloral Hydrate	Urethane	
Rat	male	Fischer	WT	adult			17 (<0.01%)		
				aged			34 (1.8%)		
			APP/PS1	adult			40 (2.2%)		
				aged			33 (1.8%)		
		Listerhooded	WT	adult				369 (19.9%)	
		Long Evans	TH-Cre	adult	20 (1%)				
		Sprague Dawley	WT	adolescent					36 (1.9%)
				adult		61 (3.3%)	78 (4.2%)	254 (13.7%)	16 (<0.01%)
			Parkinsonian	adult			18 (<0.01%)		
		Wistar	WT	adolescent					32 (1.7%)
				adult			120 (6.5%)	96 (5.2%)	
	female	Fischer	WT	adult			28 (1.5%)		
				aged			44 (2.4%)		
			app/ps1	adult			18 (<0.01%)		
				aged			26 (1.4%)		
		Sprague Dawley	WT	adolescent					28 (1.5%)
				adult		6 (<0.01%)	65 (3.5%)	3 (<0.01%)	
			dyskinetic	adult			49 (2.6%)		
			Parkinsonian	adult			90 (4.9%)		
Mouse	male	C57/Bl6	WT	adult		19 (0.1%)	5 (<0.01%)	13 (<0.01%)	53 (2.9%)
			DBH-Cre						11 (<0.01%)
			DSP-4				12 (<0.01%)		
		129S2/SvPas	VGAT-Cre						22 (1.2%)
	female	C57/Bl6	WT		15 (<0.01%)		28 (1.5%)		17 (<0.01%)
			DBH-Cre						6 (<0.01%)
			DSP-4				19 (0.1%)		
		129S2/SvPas	VGAT-cre						13 (<0.01%)
Non-human Primate	male	-	WT	adult	41 (2.2%)				

Overview of the statistical model used to assess impact of different factors on LC firing rates

We analyzed firing rate using a negative binomial regression model to explain the individual and combined effects of species, sex, age, genotype, and brain state or experimental preparation type (e.g., awake, anesthesia of various types, or *ex vivo* slice recordings). We first examined the main effects of individual factors and considered interactions between these factors (**Supplemental Table 1A & B**). Animal strain was not included in the model because strain could be completely encompassed by another factor, in this instance species (i.e. Fischer animals are only in rats, C57Bl/6 animals are only mice). For similar reasons, the interactions between age and species (adolescent and aged neurons were only obtained from rats), age and anesthesia (aged animals were all recorded under chloral hydrate anesthesia while all adolescent animals were recorded in slice), species and genotype (specific genotypes came from the

same species, such as APP/PS1 animals all being rats), and genotype and anesthesia (neurons from specific genotypes were recorded under the same anesthetic) could not be estimated.

We report effect sizes with 95% confidence intervals (CIs) as a change in firing rate (spikes/sec) to provide an intuitive quantification of how much firing rate differs between factors (Calin-Jageman and Cumming, 2019a, b; Ho et al., 2019). Importantly, small effect sizes of even 0.5 spikes/sec may carry considerable relevance to brain function. First, consider that the baseline discharge of LC neurons is already low (typically ranging from 0.5 to 5 spikes/sec) and that a relative change of 0.5 spikes/sec is a large difference in this range of activity. Second, our rudimentary understanding of how LC firing rate alters nervous system function largely precludes making a judgement regarding what effect size may (or may not) have consequences.

Activity in awake animals is reproduced in anesthetized and slice preparations, but is dependent on sex and species

Given the technical challenges of targeting the LC with recording electrodes and sustaining recording signal quality, many recordings that form substantial basis of our understanding of LC activity have been made in anesthetized animals or in brain slices. However, understanding the function of LC neuronal activity relies on how closely these preparations reflect LC activity in awake animals. The pooled dataset allowed us to address the translatability of anesthetized and slice preparations by assessing whether LC firing rates were dependent upon the recording preparation being *ex vivo* (deafferenated slice), anesthetized (chloral hydrate, urethane, or isoflurane anesthesia), or awake. This analysis considered recordings in rats and mice, for which we had both ex vivo and in vivo data. The analysis controlled for the covariates of age, sex, and species as well as genotype and brain state. There was a main effect of experimental preparation ($p<0.0001$; **Figure 2A**; **Supplemental Table 1A**). Pairwise comparisons showed that firing rates recorded under urethane were lower than those recorded under chloral hydrate ($p<0.0001$), isoflurane ($p=0.006$), and in slice ($p=0.003$) (**Figure 2A**; **Supplemental Table 2**). The effect sizes were between 0.3 and 0.47 spikes/sec (**Figure 2A**). Our analysis shows that, although there is a difference in firing rate between urethane and the other anesthetics, the firing rates of neurons in the awake state were similar to those recorded under anesthesia and in the deafferenated brain slice. Therefore, anesthetized and slice preparations seem to be reasonable proxies for spontaneous baseline activity in the awake animal.

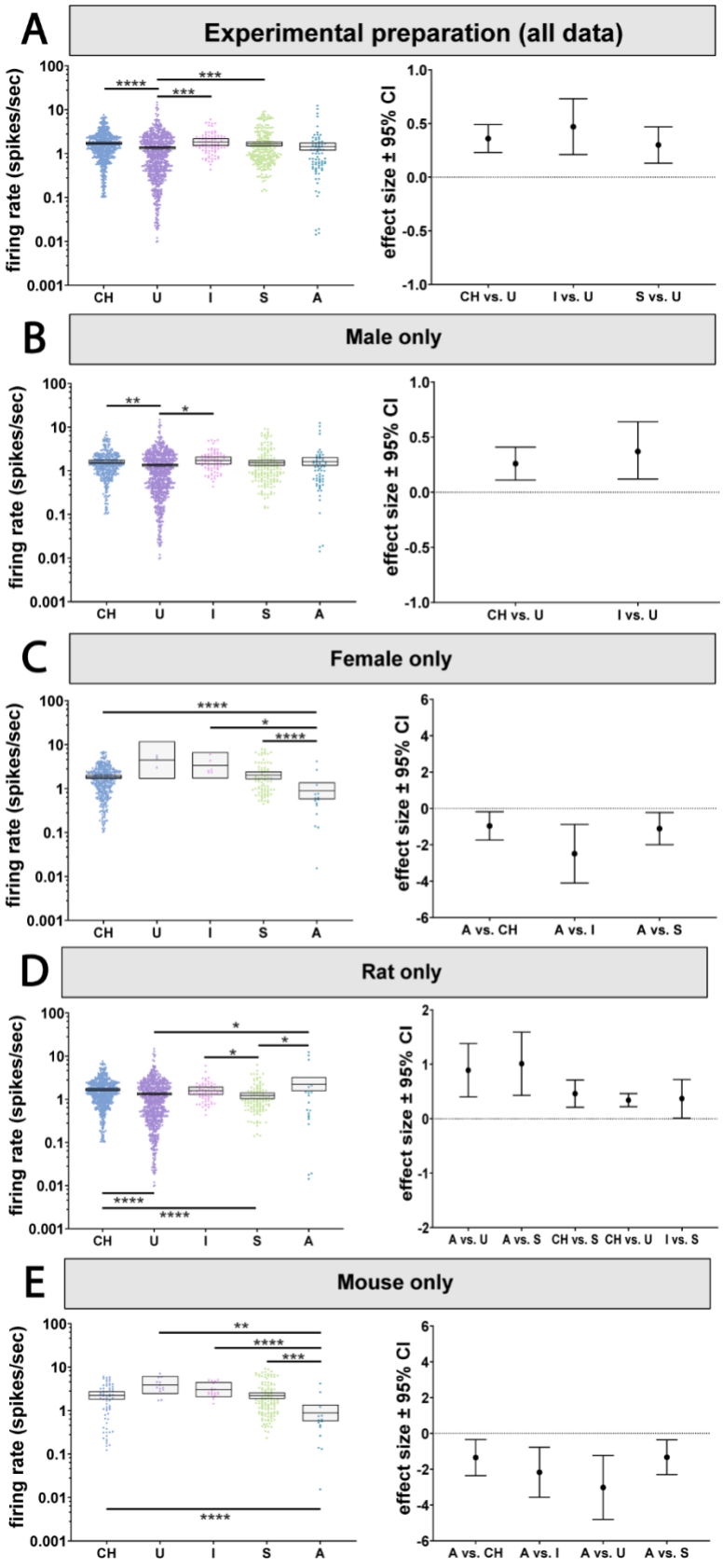

Figure 2. Baseline LC firing rates are largely consistent across brain states but interact with sex and species. A) We observed a main effect of state on LC firing rates which revealed firing rates recorded under urethane anesthesia was lower than those recorded under chloral hydrate, isoflurane, and in slice. **B)** LC firing rates under urethane anesthesia were lower than chloral hydrate anesthesia and isoflurane anesthesia in male animals. **C)** In female animals, firing rate was lower in awake animals compared to chloral hydrate or isoflurane anesthesia and to slice. **D)** In rats, LC firing rates in the awake state were higher compared to those recorded under urethane anesthesia or in slice preparations. In addition, firing rates under chloral hydrate anesthesia were higher than in slice and urethane. Finally, firing rates under isoflurane anesthesia were higher than those recorded in slice preparations. **E)** In mice, LC firing rates recorded in the awake state were lower than in all other states. *p < 0.05, **p < 0.01, ***p < 0.001, ****p < 0.0001.

However, when considering sex as an effect modifier along with state, differences emerged between anesthetized or slice preparations and awake animals. Our analysis revealed an independent interaction between recording preparation and sex (p=0.004; **Figure 2B & C**; **Supplemental Table 3A & B**). In males, activity was similar across anesthetized, slice and awake animals except for small differences in firing rate between different types of anesthesia (**Figure 2B**; see **Supplemental Table 3A** for pairwise p-values). Intriguingly, in females, LC activity during wakefulness was reduced compared to slice recordings and most anesthetics tested (**Figure 2C**; see **Supplemental Table 3B** for pairwise p-values). The effect sizes compared to the awake state varied from 0.96 to 2.49 spikes/sec. Therefore, anesthetized and isolated brain slice recordings may be appropriate proxies for awake recordings in male animals, while in females, LC neurons recorded under anesthesia or from slice are more active compared to recordings from awake animals. This change in baseline activity is large (~1 spikes/sec or greater).

The choice of species also impacted whether activity in anesthetized or slice preparations resembled awake activity. Since the dataset did not contain data from anesthetized NHPs or NHP brain slices, our analysis of the interaction between species and experiment preparation was limited to rats and mice. The statistical model indicated an independent interaction between experimental preparation and species (p=0.001; **Figure 2D & E**; **Supplemental Table 3C & D**). In rats, LC neurons from awake animals were more active than those recorded under urethane (p=0.034) or from brain slices (p=0.019). The awake rat LC firing rates were closer to (and not significantly different from) those recorded under chloral hydrate. Firing rates recorded in rats under chloral hydrate, like those recorded in awake rats, were higher than those recorded under urethane (p<0.0001) or in slice preparations (p<0.0001). Like chloral hydrate preparations, rat LC neurons recorded under isoflurane had firing rates that were higher than those recorded in slice (p=0.05) and, accordingly, were more similar to activity in the awake rat (**Figure 2D**; **Supplemental Table 3C**). Thus, in comparison to awake rats, *ex vivo* and urethane recordings are

associated with suppressed LC activity, while LC activity under chloral hydrate and isoflurane anesthesia was similar to awake activity.

Surprisingly, mice showed a largely opposite pattern relative to what was observed in rats. Whereas LC neurons were more active in awake rats (compared to some other preparations), awake mouse LC neurons were less active than all other preparations covered by our data set. Specifically, the LC firing rate in awake mice was lower than LC activity under chloral hydrate ($p<0.0001$), isoflurane ($p=0.0005$), or urethane ($p=0.001$), or slice recordings ($p<0.0001$) (**Figure 2E**; **Supplemental Table 3D**). The opposition between rats and mice is apparent in the effect size plots (**Figure 2D & E**), which show positive effect sizes for rats and negative effect sizes for mice.

Sex impacts baseline LC firing rates in opposing directions based on state and species

Biological sex is associated with differences in autonomic control, the stress response, sleep, and cognition, as well as symptoms of various clinical disorders (Brady and Randall, 1999; Whitacre, 2001; Kessler, 2003; Tolin and Foa, 2006; Lovejoy et al., 2009; Appelman et al., 2015; Bangasser et al., 2016; Ferretti et al., 2018; Poe et al., 2020). We wondered whether these sex differences could be associated with sex-specific LC firing rates. A recent study has shown that brain slice recordings of LC neurons from female mice are more excitable than those from males (Mariscal et al., 2023). However, a systematic comparison of male and female LC firing rates has not been done previously, nor has the interaction of sex with other factors such as species or experimental preparation type been studied. Our analysis revealed a main effect of sex on firing rate ($p<0.0001$; **Figure 3A**, **Supplemental Table 1A and 4**). We found that the female LC was more active than male LC with an effect size of 0.4 spikes/sec. However, there was also an independent interaction between sex and state ($p=0.0044$; **Figure 3B-D**; **Supplemental Table 1B**). Specifically, the female LC was only more active when recorded under chloral hydrate ($p=0.031$) or from brain slice recordings ($p=0.024$). On the other hand, in awake animals, the female LC was actually less active compared to the male LC ($p=0.004$; **Figure 3B-D**; **Supplemental Table 5A**). The effect of sex also depended on species ($p=0.0103$; **Figure 3E & F**; **Supplemental Table 1B**). In rats, the female LC is more active than male LC ($p<0.0001$; **Figure 3E**; **Supplemental Table 5B**), whereas in mice the opposite was observed ($p=0.034$; **Figure 3F**; **Supplemental Table 5C**). While LC firing rate varies by sex, whether females have a higher firing rate depends on species and experimental preparation.

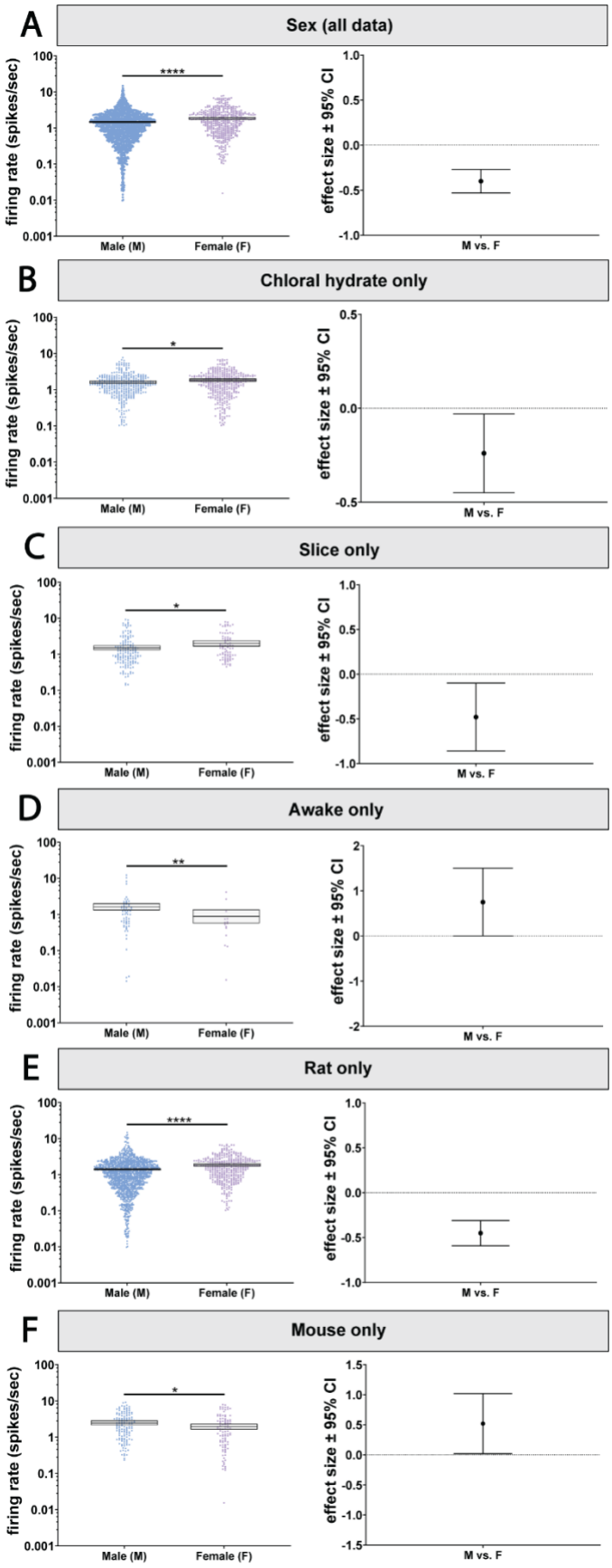

Figure 3. The effect of sex on LC firing rates depends on state and species. A) LC neurons recorded from female animals had a higher firing rate compared to males. **B)** Female animals recorded under chloral hydrate and **C)** in slice have a higher firing rate than males. **D)** Contrastingly, in male animals, LC firing rates were higher than females in the awake state. **E)** In rats, females LC firing rates were higher than in males. **F)** This effect was reversed in mice, where male LC neurons were more active than female LC neurons. *p < 0.05, **p < 0.01, ****p < 0.0001.

Baseline LC firing rates in mice differ from those in other species

Next, we turned to the effect of species on LC firing rates because it has long been assumed that LC activity is conserved across model species. Using the pooled dataset, we were able to compare, in a single analysis, the commonly studied model organisms: mouse, rat, and NHPs. Our analysis showed a significant main effect of species (p<0.0001; **Figure 4A**; **Supplemental Table 1A**). Neurons recorded from mice had higher firing rates compared to rats (p<0.0001) and NHPs (p=0.0001), but rats and NHPs did not significantly differ from each other (**Figure 4A**; **Supplemental Table 6**).

The effect of species on LC activity interacted with the type of experimental preparation defining the state of the animal (p=0.001, **Figure 4B-F**; **Supplemental Table 1B**). We compared firing rates using pairwise tests and observed that the mouse LC is more active relative to the rat LC under all tested anesthetics and during *ex vivo* recordings (**Figure 4B-E**; **Supplemental Table 7A**). However, in the awake state, mouse LC neurons were less active compared to rats (p=0.0036) and NHPs (p=0.0491) (**Figure 4F**; **Supplemental Table 7A**).

The effect of species also interacted with sex (p=0.0103; **Figure 4G & H; Supplemental Table 1B**). The higher firing rate in mice relative to rats and NHPs was observed specifically in males (p<0.0001 vs rats; p<0.0001 vs NHPs) (**Figure 4G; Supplemental Table 7B**). The effect sizes between male mice versus male rats and male NHPs were 1.09 and 1.07 spikes/sec, respectively. On the other hand, in females, there were no species-specific differences between mice and rats (**Figure 4H**; **Supplemental Table 7C**). We did not have data from female NHPs for comparison. These findings indicate that, in males, the mouse LC is more active relative to the rat and NHP LC, whereas in females LC activity is similar between rodent species. In sum, there are mouse-specific differences in LC firing rate, but those differences are in opposite directions depending on whether sex or a particular experimental preparation (awake) is considered as a variable.

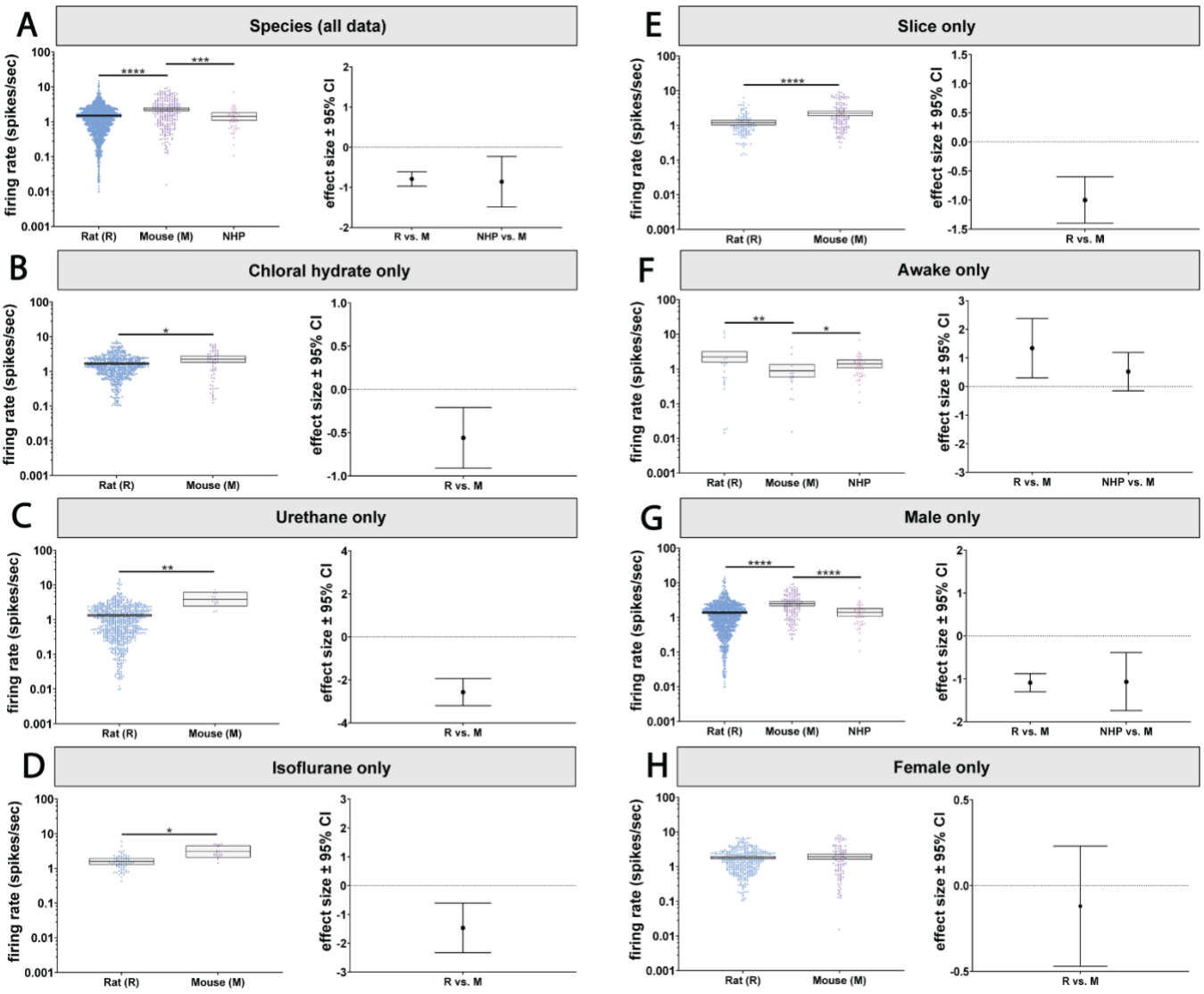

Figure 4. A main effect of species on baseline LC firing rates depends on both state and sex. A) There was a main effect of species on LC firing rates, with mouse LC neurons displaying higher activity compared to both rats and NHPs. The effect of species also depended on the state of the animal. Mouse LC neurons were hyperactive when recorded under **B)** chloral hydrate **C)** urethane **D)** isoflurane and **E)** in slice. **F)** In awake animals, this effect was reversed, with rat and NPHs displaying higher firing rates compared to mice. There was also a separate species and sex interaction. **G)** Male rats and NPHs had lower firing rates compared to mice. **H)** There was no difference between rat and mouse LC firing rates when comparing females, while we had no NHP data for comparison. *p < 0.05, **p < 0.01, ***p < 0.001, ****p < 0.0001.

Baseline LC activity is unaffected in models of neurodegenerative disease unless the degeneration specifically targets LC neurons

LC dysfunction is a universal feature of Alzheimer's disease, Parkinson's disease, and other neurodegenerative disorders beginning with the early aggregation of disease-specific proteins followed by late-stage degeneration (Weinshenker, 2018). Subsets of the pooled dataset included recordings from TgF344-AD rats that carry transgenes expressing autosomal dominant, early onset Alzheimer's disease-causing APP/PS1 mutations (Cohen et al., 2013; Kelberman et al., 2023). Importantly, these rats develop hyperphosphorylated tau in the LC prior to amyloid or tau pathology in forebrain regions (Rorabaugh et al., 2017), similar to the temporal pattern of tau deposition observed in humans (Braak et al., 2011). The dataset also included three pharmacological manipulations to induce disease-like states. The first manipulation was the selective adrenergic neurotoxin, N-(2-chloroethyl)-N-ethyl-2-bromobenzylamine hydrochloride (DSP-4), which induces LC noradrenergic axonal degeneration (Iannitelli et al., 2023). The second manipulation were rats unilaterally injected with 6-OHDA into the medial forebrain bundle to induce dopaminergic system neurodegeneration while sparing the noradrenergic system using pretreatment with desipramine (Miguelez et al., 2011a). This second manipulation produces a hemiparkisonian disease model. The third manipulation combined 6-OHDA injections into the median forebrain bundle with 3 weeks of L-DOPA treatment, which produces a dyskinetic disease model (Miguelez et al., 2011b). We asked whether these manipulations led to changes in LC firing rates that could be relevant for the presentation of neurodegenerative disorders. There was a main effect of disease model type on firing rates ($p<0.0001$; **Figure 5A; Supplemental Table 1A**). Post-hoc analysis revealed that animals treated with DSP-4 had higher firing rates than wild-type animals ($p=0.0249$; **Figure 5A; Supplemental Table 8**). Unexpectedly, LC activity did not differ from control animals in any of the other disease models.

Due to the relationship between neurodegenerative disorders and age (Hindle, 2010; Hou et al., 2019; Zaib et al., 2023), the age of the animal might interact with the preclinical models to produce a change in LC activity. However, we found that the effect of these disease models on firing rate was not dependent on sex or age (**Supplemental Table 1B**). Note that interactions with species or brain state were not estimable. Overall, our findings are unexpected given that the genetic and pharmacological neurodegenerative disease models, which presumably relate to symptoms through altered noradrenergic

neuromodulation by the LC, actually resulted in no change in baseline LC activity (with the exception of the DSP-4 pharmacological lesion model).

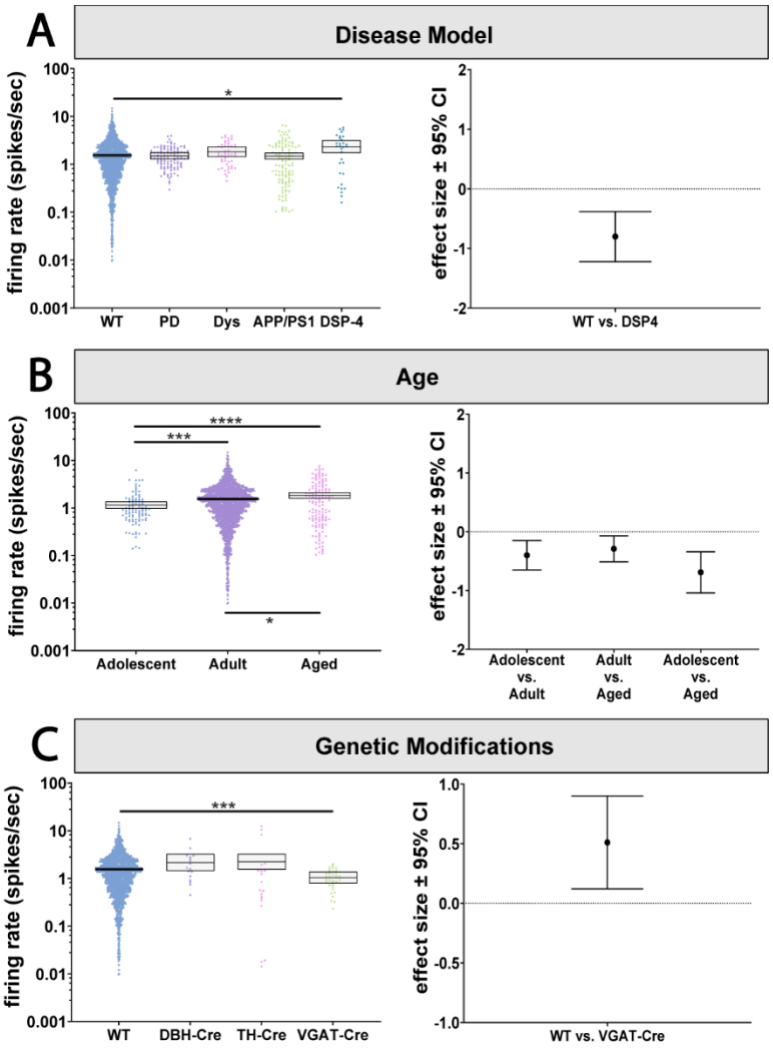

Figure 5. The effect of disease models, age, and genetic manipulations on LC firing rates. A) There was a main effect of disease model on LC firing rates and post-hoc analysis revealed that DSP-4 lesions increased LC activity. **B)** There was also a main effect of age on LC firing rates, with firing rate gradually increasing over the course of aging. **C)** There was also a main effect of genetic modification on LC firing rates, with VGAT-Cre animals demonstrating a lower firing rate when compared to WT animals. *p < 0.05, ***p < 0.001, ****p < 0.0001.

The LC becomes gradually more active over the course of aging

The largest risk for developing neurodegenerative disorders is age (Hindle, 2010; Hou et al., 2019; Zaib et al., 2023). Moreover, age heavily impacts LC structure and function. For example, studies in human subjects demonstrate that although there is no age-related loss of LC cell bodies (Theofilas et al., 2017),

there are changes in LC functional connectivity and neuromelanin signal intensity across aging (Zhang et al., 2016; Liu et al., 2020), However, preclinical studies have reported LC cell body and axon loss over the course of aging (Sturrock and Rao, 1985a; Rorabaugh et al., 2017; Kelberman et al., 2022). LC firing rates have not been compared over the course of aging in a large dataset in any species. Therefore, we investigated whether there were any changes in LC firing rates during the process of normal aging. Rodents were designated as adolescent (<3 months), adult (3-12 months), or aged (>12 months), while all NHP data came from adult animals (10-16 years) (Dutta and Sengupta, 2016; Simmons, 2016; Colman, 2018; Chiou et al., 2020; Wang et al., 2020; Delage et al., 2021). There was a main effect of age on firing rates ($p=0.006$; **Figure 5B**; **Supplemental Table 1A**). Adolescent firing rates were lower than both adult ($p=0.0002$) and aged animals ($p<0.0001$), while LC activity in adults was lower than in aged animals ($p=0.035$) (**Figure 5B**; **Supplemental Table 9**). Note that the interaction of age with species and state were not estimable (**Supplemental Table 1B**). Assessing the other factors revealed no interaction between age and any other factor, suggesting that the gradual increase in LC activity during aging is not genotype- or sex-dependent. Thus, LC firing rates gradually increase with age, which has implications for understanding the contributions of LC activity to behavioral changes during aging and disease prevalence during aging.

Brain-wide Cre expression in GABA interneurons is associated with a less active LC relative to wild-type rats and mice

Optogenetics and chemogenetics are commonly used in neuroscience. The assumption is that the requisite genetic modifications that enable optogenetics and chemogenetics (such as expressing Cre recombinase in all catecholaminergic neurons or in all GABA neurons throughout the brain) have no effect on LC activity. We compared recordings from *(i)* dopamine beta-hydroxylase (DBH)-Cre mice, which express Cre in noradrenaline-producing neurons (Breton-Provencher and Sur, 2019; Breton-Provencher et al., 2022; Dvorkin and Shea, 2022); *(ii)* vesicular GABA transporter (VGAT)-Cre mice, which express Cre in GABAergic interneurons (Vong et al., 2011; Kuo et al., 2020; Breton-Provencher et al., 2022); and (iii) tyrosine hydroxylase (TH)-Cre rats, which express Cre in all catecholaminergic (dopaminergic and noradrenergic) neurons (Witten et al., 2011; Uematsu et al., 2017). There was a significant effect of the type of genetic manipulation on firing rates ($p<0.001$, **Figure 5C**; **Supplemental Table 1A**). Post-hoc testing demonstrated that wild-type animals had higher firing rates compared to VGAT-Cre animals ($p=0.0007$) but were not different from DBH-Cre or TH-Cre animals (**Figure 5C**; **Supplemental Table 9**). The effect of these genetic manipulations was not dependent on age or sex.

Note that we could not assess any interaction effects with state or with species because VGAT-Cre and DBH-Cre data were in mice, while TH-Cre data were in rats) (**Supplemental Table 1B**). This result shows that a widely used genetic modification that merely enables optogenetic or chemogenetic manipulation of GABAergic interneurons throughout the brain can reduce LC activity on the order of 0.51 spikes/sec compared to wild-type animals. Given the overall low frequency of baseline LC activity, this change in spike rate is substantial. Importantly, this change is not due to manipulation of GABAergic interneuron activity, but due only to expressing Cre recombinase in them.

Phasic, burst firing of LC neurons occurs spontaneously and shows multiple burst patterns

In the preceding analyses, we used a pooled dataset of 1,855 LC neurons to demonstrate that time-averaged baseline firing rate depends on factors such as sex, species, age, brain state (defined by type of experimental preparation), disease model, and genetic manipulation. It is possible that these factors also affect the *temporal patterns* of spiking. LC neurons, like dopaminergic neurons (Grace and Bunney, 1984) have been characterized as emitting spikes in two patterns: tonic baseline activity or evoked phasic bursts (Foote et al., 1980; Aston-Jones and Bloom, 1981b; Grant et al., 1988; Harley and Sara, 1992; Aston-Jones et al., 1994; Coull, 1998; van den Brink et al., 2016a). The tonic spiking mode encompasses baseline firing discussed above, canonically at rates below 6 spikes/sec with ISIs lasting several hundreds of msec resulting in slow, irregular spike discharges. The phasic mode consists of internal or external stimulus-evoked activations of 2-3 spikes within a 50-100 msec window (Aston-Jones and Bloom, 1981b; Neves et al., 2018) and correspondingly short (<80ms) ISIs (Tung et al., 1989; Miguelez et al., 2011a). We sought to determine whether LC neurons spontaneously burst without external triggers, and to characterize those spontaneous burst patterns. We expected occasional phasic bursting in awake recordings that was less pronounced or absent in other preparations. We also expected that phasic busting would be a canonical train of 2 to 3 spikes with an ISI histogram peak time of less than or ~ 80 msec followed by a long tail of larger ISIs. Our key prediction was that neurons with phasic bursts would cluster together with a similarly low ISI time in a consistent pattern.

We tested this prediction by clustering ISI distributions across neurons. To do so, we performed principal components analysis (PCA) on the ISI distributions (20 msec bin size, range from 0 to 2.5 sec), which permits clustering of similar distributions among sub-sets of 1,708 neurons (see exclusion criteria from **Figure 1**). We then performed kmeans clustering (see methods) on the resulting component scores for PC1 through 6, which together explained ~75% of the variance in ISIs (**Supplemental Figure 2**). Prior to

clustering, we used a gap test to assess the optimal number of clusters (k) between 1 and 20 clusters. The optimal K was 17 clusters of ISI distributions across the 1,708 neurons (**Figure 6A; Supplemental Table 10**). Each cluster contained multiple neurons with similar ISI distributions. The number of neurons assigned to each cluster is shown in **Supplemental Table 10**. The four example ISI distributions in **Figure 6A** show the across-neuron average ISI distribution for clusters 1,5,6, and 12.

It is apparent in the examples that some neuronal clusters have ISI distributions that are relatively flat with large variance (e.g., cluster 12 in **Figure 6A**), which indicates irregular firing. Conversely, other clusters had narrow distributions (e.g., clusters 1 and 5 in **Figure 6A**), which indicates more rhythmicity in spike times. We also noted that the ISI distributions of different neuronal clusters peaked at different times. Some distribution peak times correspond to bursting (e.g., peak at 50 msec, cluster number 3, **Supplemental Table 10**), whereas others correspond to irregular baseline firing (e.g., peak at 760 msec, cluster number 14, **Supplemental Table 10**). In sum, there were two apparent characteristics that distinguished ISI distributions from each other: peak time and variance.

We captured these two characteristics by calculating the kurtosis of the across-neuron average ISI distribution for each neuronal cluster, and then plotting it against its mean (distribution peak) ISI (**Figure 6B**). Kurtosis was used to capture the “tightness” of the ISI distribution, and thus its degree of rhythmicity with tighter distributions having more similar ISIs (i.e., more rhythmicity). Kurtosis is a mathematical characteristic of a distribution that describes the shape of the distribution, especially with respect to its tailedness. A normal distribution has kurtosis of 0. Negative kurtosis describes a distribution with more outliers which is therefore flatter and wider than a normal distribution. Positive kurtosis is “tighter” than normal distribution, in that it has less outliers (less tailedness). Positive kurtosis can be thought of as more ISIs concentrated around the mean ISI, and thus more rhythmicity in spike times. Neuronal clusters, when inspected on the joint basis of kurtosis and mean ISI, fell into 3 groups. Group 1 (**Figure 6C)** was rare (2.75% of LC neurons) with an ISI peak that was short duration (50 msec to 150 msec) and very high kurtosis indicating highly rhythmic firing with short ISIs. ISIs of neuronal clusters in Group 1 were narrowly distributed around 50, 110, 120, and 150 msec (clusters 3, 2, 4, and 1 respectively). The second group made up of 29.39% of LC neurons (**Figure 6D**) also had low ISI peak values (40 msec to 320 msec) and high kurtosis (although lower than group 1) indicating a somewhat narrow distribution. The ISI distributions of the neuronal clusters in Group 2 indicate that, relative to Group 1 and 3, firing is semi-rhythmic. Some of the neuronal clusters in Group 2 preferred to spike with a 40 msec ISI (cluster 6) or an 80 msec ISI (cluster 7) illustrating spontaneous phasic burst firing exhibited by different populations

of neurons. Moreover, other clusters in Group 2 had peaks at 210, 230, and 320 msec (clusters 11, 5, and 9, respectively) and might be considered tonic firing with somewhat more regularity in spike times compared to Group 3. Finally, most LC neurons (67.86%) fell into the third group (**Figure 6E**) with kurtosis values of nearly 0 or negative kurtosis. This group is, therefore, irregular firing. The ISI peak in this group ranged from 170 msec to 1050 msec. In contrast to the classic two-mode tonic-phasic framework, we show that multiple non-evoked phasic burst firing patterns spontaneously occur in different sets of LC neurons. Importantly, we found a stark difference in prevalence of firing patterns across the data set. Two-thirds of the neurons fired in irregular patterns and one third fired in fast, semi-rhythmic patterns. However, merely 47 neurons (2.75%) fired in fast rhythmic patterns. Individual studies of small sample size would likely fail to detect or differentiate between such patterns. We next turned to assessing how these newly identified firing patterns, which are expressed by different neuronal clusters, mapped onto various traits (i.e., sex, species, age, brain state, disease model, and genetic manipulation).

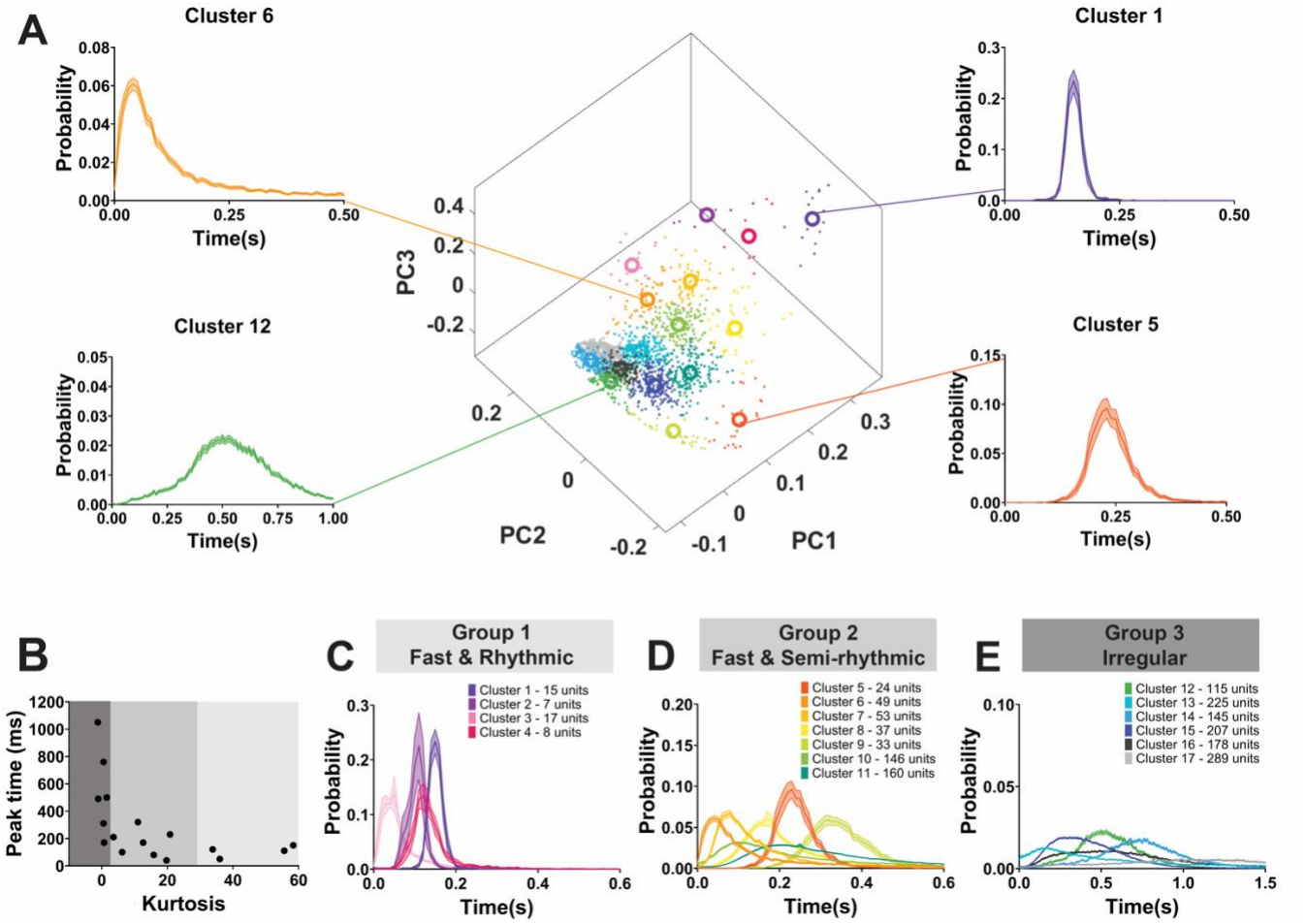

Figure 6. LC neurons have varied temporal patterns of activity that can be broadly categorized into 3 groups

A) PCA space showing the 17 clusters identified by using kmeans clustering and principal components analysis on 1708 neurons' ISI distributions. Average ISI distribution for 4 example clusters (clusters 1,5,6, and 12) are shown (right and left). Cluster identity is highlighted using color. **B)** Further grouping of clusters based on average cluster traits identified three separate groups. Scatterplot of each cluster's kurtosis and maximum probability ISI time identified 3 groups – **C)** Group 1; fast and rhythmic, **D)** Group 2; fast and semi-rhythmic, and **E)** Group 3; irregular. ISI distributions of all clusters in each group are shown for groups 1-3 **(C-E)**. Figure legends show the color of each cluster and how many neurons are contained in each cluster.

Species, age, and brain state were associated with specific spike timing patterns, but males and females expressed similar patterns

Among the 17 clusters identified by PCA, we assessed whether any traits (sex, species, age and brain state) were preferentially expressed by specific clusters. We compared the proportion of each trait in each cluster to their proportion in the overall population of neurons included in this study. The difference was compared using a chi-squared test, and the test statistics and p-values are shown in **Supplemental**

Table 11. We observed differential expression of ISI patterns according to species and age, but not sex. Mouse neurons had a higher presence in clusters 1, 5, and 9 that expressed rhythmic or semi-rhythmic firing patterns. Rats had a higher representation of neurons in clusters 11,15, and 16 with greater irregularity in ISIs. Cluster 16 also had an increased proportion of neurons from NHP (**Figure 7A**). ISI distributions of clusters with a higher proportion of mouse neurons were less variable on average compared to clusters with a higher proportion of rat neurons (**Figure 7A, lower right insert**). Regarding age, clusters 3, 6, 7, and 10 showed shorter peak ISIs and skewed older with more neurons from aged animals and fewer from adolescent animals. Irregularly distributed ISIs in clusters 15, 16, and 17 were almost entirely comprised of neurons from adults. Finally, clusters 5, 9, and 12 that contained longer peak ISI times, skewed younger with more neurons from adolescent animals and completely lacked neurons from aged animals (**Figure 7B**). ISI distributions from clusters with higher proportions of aged animals showed shorter ISIs compared to clusters with high proportions of adult or adolescent neurons (**Figure 7B, lower right insert**). Despite these strong trait-associated firing patterns, sex did not appear to associate with any particular ISI distribution except for cluster 7, which had a higher proportion of neurons recorded in females (**Figure 7C**).

We also observed clusters of ISI distributions that differed in their composition of neurons based on brain state (awake, anesthetized, or *ex vivo* recording). Clusters 1, 2, 4, 5, 9, 12, and 14 were comprised of significantly more neurons from, anesthetized and brain slice recordings than the overall population (**Figure 7D**). Neurons recorded under anesthesia were the predominant contributors to clusters 11, 15, and 16. Clusters 10 and 13 had a higher proportion of neurons from awake animals with very few neurons recorded *ex vivo*. Clusters with higher proportions of neurons recorded *ex vivo* were less variable and had lower ISIs, especially when compared to clusters with more awake or anesthetized animals which had much more variable ISI distributions (**Figure 7D, lower right insert**). Given the over-representation of neurons recorded under anesthesia in some clusters, we further explored the effect of anesthesia by comparing the proportion of different types of anesthesia (urethane, chloral hydrate, or isoflurane) in each neuronal cluster. Clusters 6, 7, and 10 had a predominance of neurons recorded under chloral hydrate, while neurons recorded under isoflurane were absent. Clusters 12 and 14 also had a greater proportion of neurons recorded under isoflurane compared to the overall population. Clusters 11 and 16 had a higher proportion of neurons recorded under urethane (**Figure 7E**). These findings show that specific experimental preparations were associated with particular ISI patterns. However, diverse firing patterns, including multiple burst patterns, were found across each preparation.

Neurodegenerative models expressed different patterns of spike timing compared to wild-type animals

We wondered whether models of neurodegenerative disease (either due to genetic modification or pharmacological manipulation of the LC noradrenergic system) might also be associated with particular spiking dynamics. Neuronal clusters 6, 10, and 13 were highly enriched with neurons recorded from APP/PS1 genetically modified animals, but those same clusters included very few (or were devoid of) neurons from parkinsonian and dyskinetic pharmacological models. On the other hand, we observed the opposite pattern in clusters 14 and 17, which had a greater proportion of neurons recorded from parkinsonian and dyskinetic animal models with hardly any representation of the APP/PS1 animal model (**Figure 7F**). ISI distributions from clusters with a higher proportion of APP/PS1 recorded neurons were shifted toward shorter ISIs and were less variable than the ISI distributions associated with parkinsonian animal models (**Figure 7F, lower right insert**). Thus, we found that models aimed at replicating core features of neurodegenerative diseases often expressed different LC spike timing patterns.

Genetic modification for opto/chemo-genetic manipulation was associated with altered spike timing

We investigated spike train dynamics across Cre-expressing animals. Cluster 10 had a higher proportion of neurons recorded from DBH-cre and VGAT-cre animals. Cluster 13 was comprised of a higher proportion of VGAT-cre, DBH-cre, and TH-cre animals compared to the overall population of neurons. Perhaps most strikingly, neurons recorded in TH-cre animals were nearly exclusively found in cluster 3 and were only found in clusters 3 and 13 (**Figure 7G**). Overall, these results suggest that genetic manipulation of LC neurons or GABA interneurons to introduce Cre expression may be associated with changes in the temporal spike patterns of LC neurons.

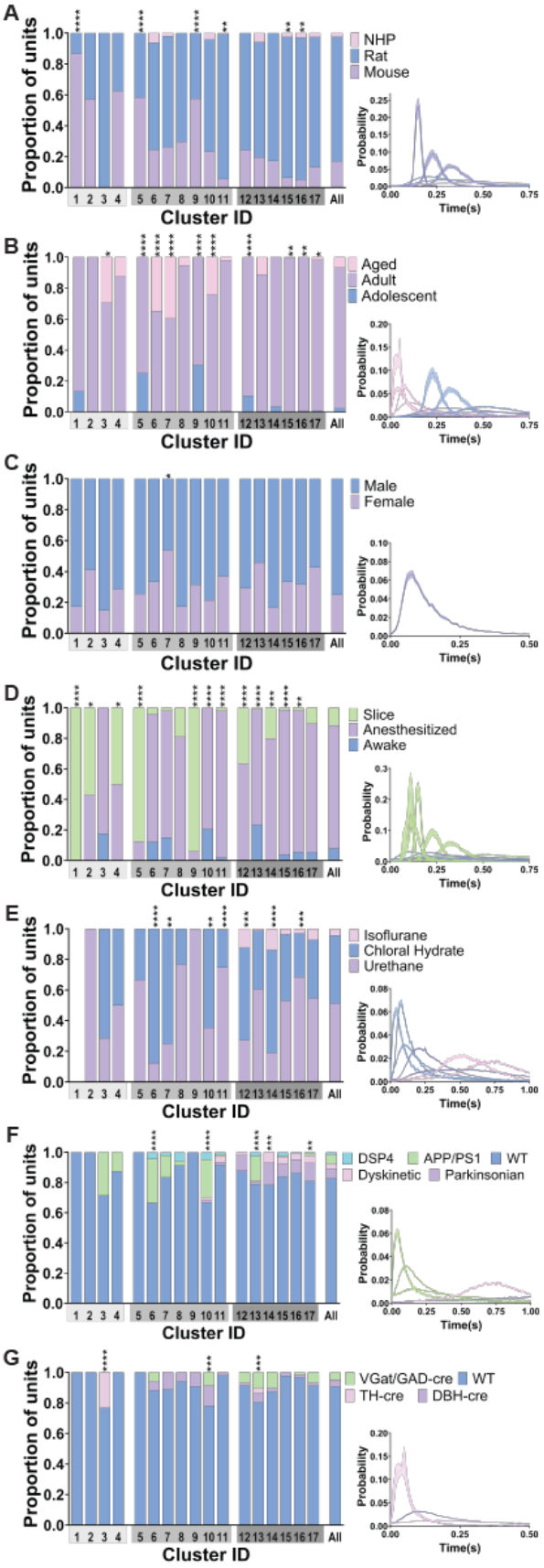

Figure 7: Traits such as species, age, and recording preparation were represented differently across the 17 clusters based on ISI distributions. Bar graphs show the proportion of traits represented in each of the 17 clusters (cluster ID on x axis) and the population as a whole (rightmost bar). Gray shading under each cluster number identifies which group those clusters belong to (from Figure 14C-F). Mean ISI distribution of the clusters with a significantly different composition of traits compared to the overall population of neurons (chi squared) are shown in the lower right inserts. The color of the ISI distribution corresponds to the trait that is most overrepresented in the cluster (identified by the largest fold change in proportion, ((proportion in cluster-proportion in population)/proportion in population). **A)** Species were differentially represented across the 17 clusters. Clusters 1, 5, and 9 had an overrepresentation of mouse neurons. ISI distributions of these clusters were less variable than clusters with higher proportion of neurons from rats (11 and 15) or NHP (16). **B)** Clusters showed distinct differences in their composition based on age. Clusters 3, 6, 7, and 10 were comprised of more aged neurons and displayed shorter ISIs than clusters 5, 9, and 12 which consisted of a greater proportion of adolescent neurons. Clusters 15, 16, and 17 had a greater proportion of adult neurons with increased variability in their ISI distributions. **C)** Sex was equally represented in all clusters except for cluster 7 which had increased female neurons compared to the population. **D)** 70% of clusters had statistically different proportions of neurons based on state compared to the population, a large majority of which had a greater proportion of neurons from *ex vivo* preparations. Clusters 1, 2, 4, 5, 9, 12, and 14, had a larger proportion of neurons from reduced preparations. Clusters 11, 15, and 16 had more neurons from anesthetized animals. There was an increased proportion of neurons from awake animals in clusters 10 and 13. Both anesthetized and awake clusters showed increased ISI variability compared to clusters with a majority of *ex vivo* recorded neurons. **E)** Anesthesia type was differentially represented in 7 clusters. Neurons recorded under chloral hydrate were overrepresented in clusters 6, 7, and 10 which had ISI distributions with little variability and low ISIs. Clusters 12 and 14 had a greater proportion of neurons recorded under isoflurane and the proportion of neurons recorded under urethane anesthesia was increased in clusters 11 and 16. **F)** Clusters 6, 10, and 13 had a higher proportion of neurons from APP/PS1 animals. These clusters had lower ISIs compared to the clusters with increased neurons from parkinsonian (cluster 17) or dyskinetic (cluster 14) animals. **G)** Neurons from genetically modified animals for opto/chemo-genetic manipulation were differently represented in clusters 3, 10, and 13. TH-cre animals were only found in clusters 3 and 13; and were almost all in cluster 3. Cluster 10 had an increased proportion of neurons from DBH-cre animals.

Second order statistics of LC spiking is diverse and varies greatly across neurons

We characterized the second order statistics of LC neuronal spiking using so-called “return maps” or “Poincaré maps,” which are visualizations of the joint relationship between successive interspike intervals. This analysis provides important information on how the variability in temporal firing patterns is organized. The return map can show temporal patterns that are not apparent in the raw data, including stable states (attractors) of neuronal firing (Siegel, 1990; Carlson and Foote, 1992; Szücs et al., 2005). For instance, **Figures 8A and 8B** show synthetic data for two neurons, one which fires regularly and the other which fires tonically with occasional bursts. The return map distinguishes these two patterns and provides an intuitive visualization of the second order statistics of spike trains. Here, we calculated return maps for the 1,708 LC neurons (which met requisite conditions for ISI analysis). We observed several unique

spiking patterns, which we manually grouped. Finally, we assessed how distinct types of second-order firing patterns mapped onto various factors.

We identified unique patterns in the 1,708 neurons in the return map density plots and manually grouped them into 8 types. **Figures 8C-J** shows an example unit from each of these 8 types of return maps, in which distinguishing features are visible. Types 1 - 5 (accounting for 62.5% of the patterns produced and most neurons) show a single stereotyped firing pattern (i.e, an attractor) with different shapes due to ISI variability **(Figures 8C-G)**. This pattern is expected from irregular tonic baseline activity. For example, the return density plots of type 1 and 4 are both evenly distributed around a common mode ISI value but the variability in type 1 is larger than type 4, which is highly discrete and the result of extremely regular activity similar to the synthetic raster used in Figure 8A. Types 6, 7, and 8, however, have multiple attractors that also differ in their shape and variability **(Figures 8H-J)**. The neurons with multi-attractor firing patterns are generated by tonic firing interspersed with bursting at discrete relative frequencies. This identifies specific relative relationships in spontaneous bursting activity of LC neurons. The number of units in each type varied from 21 to 689. More complex multi-attractor firing patterns were observed in a minority of neurons (n=115, 6.73%), while most neurons fired in type 1 or type 2 single-attractor patterns (n=1249, 73.13%). Descriptive values for each type can be found in **Supplemental Table 12**. These findings show that LC neurons produce firing patterns that are stereotyped attractors, and some neurons display transitions between multiple attractors. The attractor landscape is diverse across LC neurons. Therefore, we wondered whether these activity landscapes mapped onto particular factors, such as species, sex, etc.

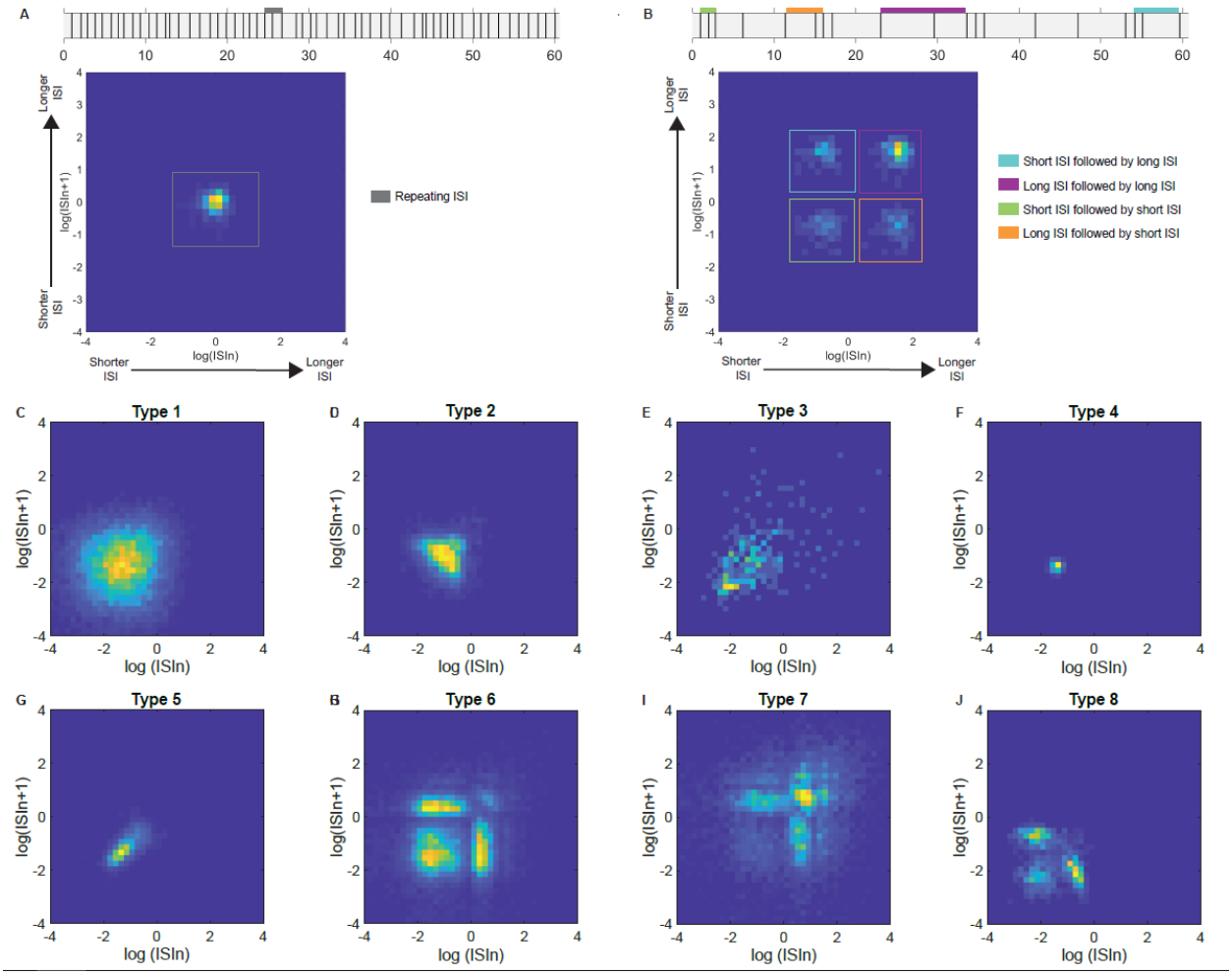

Figure 8: Return density plots identify distinct higher order temporal dynamics of ISIs in 8 patterns. Return density plots show the relationship between pairs of ISIs in a single neuron, namely the ISI of a given neuron on the x-axis against the following ISI of that same neuron on the y-axis. The frequency in which those relationships occur for a given unit are represented in the color where blue is no/infrequent ISI pairings and yellow is a pairing that occurs often. **A&B)** Example neurons with their respective raster plot (top) and return density plots (bottom) show the relationship between firing rate, ISI, and return density plots. **A)** Example neuron with a regular/tonic firing rate results in a return density plot with one point. **B)** Another example neuron with periods of tonic firing along with bursts results in a return density plot with a distinct shape of four points. Burst firing is highlighted in green in the raster and return density plot. Short ISIs followed by long ISIs (blue) and long ISIs followed by short ISIs (orange) are represented in the upper left and lower right corners of the return density plot. Tonic firing, long ISI followed by long ISIs, are highlighted in purple in the raster plot and return density plot. **C-J)** Return density plot for the manually identified patterns fell into these 8 types. **C-G)** Types 1-5 (**C:** n=689; **D:** n=560; **E:** n=90; **F:** n=206; **G:** n=48) show single attractor patterns, likely representing different forms of irregular tonic baseline activity. **H-J)** Return density plots for type 6-8 (**H:** n=44; **I:** n=50; **J:** n=21) contain multiple attractors, from 3-5, and have differences in the number of attractors, gaps between attractors, and variability in the attractors. These types likely represent tonic and spontaneous phasic burst firing occurring in baseline LC activity.

Species-, age-, and sex-specific second-order spike train statistics

We characterized to what degree different factors were expressed in each return map type by comparing the proportion of neurons with a specific trait to the overall population (**Supplemental Table 13**). We begin with the contribution of species, age, and sex. Our analysis revealed that some firing patterns are almost entirely expressed by a single species (**Figure 9A**). Type 2 (single attractor) was almost exclusively rat LC neurons. Types 4 and 5 (single attractor) had a greater proportion of neurons from mice and rarely included neurons recorded from NHPs. However, NHP LC neurons were overrepresented in type 3 (single attractor), which also contained a large proportion of mouse LC neurons. Therefore, we found species specific variations in tonic baseline firing intervals from mouse, rat, and NHP LC.

We also examined the effect of age on LC spike train dynamics (**Figure 9B**). Type 1 and 3, single attractors with wide variability, had a higher proportion of aged animals. Adolescent neurons were especially common in type 4 which showed the most consistent ISIs. Type 2 was almost entirely made up of adult neurons with little/no adolescent or aged neurons. Thus, the adult LC may express a specific tonic firing pattern that distinguishes it from tonic activity patterns in adolescence or later life. Of note, variability (spread) between relative ISIs (**Figure 8C-F)** is very low in the type with more adolescent animals (**Figure 8F**; type 4**),** increasing in the adult animal type **(Figure 8D**; type 2**)**, and aged animal types showing the greatest variability **(Figures 8C&E**; types 1 and 3**)**. Thus, distinct timepoints in development and aging are associated with specific relative LC neuronal firing patterns.

Lastly, we investigated whether firing patterns were expressed to a greater extent in males compared to females and vice versa (**Figure 9C**). However, no return map type was entirely specific to one of the sexes. Male neurons predominated type 1 and 7, whereas type 4 had a higher proportion of female neurons. These results show that sex has some influence on higher-order LC spike train patterns, but all relative patterns are expressed in both sexes.

Specific second order spike train dynamics are expressed in slice, anesthetized, and awake recordings

We next examined the role of experimental preparation on second order dynamics. Type 4 and 5 return maps (single attractor, limited variability) had a significantly higher proportion of neurons recorded in a slice preparation and contained no neurons recorded in awake animals. Type 2 (single attractor) was almost entirely made up of neurons from anesthetized animals. Finally, type 1 (single attractor) and 8 (multiple attractors) were comprised of a higher proportion of neurons recorded in the awake state with

a lower proportion of neurons recorded in the slice preparation (**Figure 9D**). These results suggest that the preparation in which LC neurons are recorded is associated with specific second-order spike train statistics.

Given that experimental preparation is associated with altered LC spike train dynamics, we assessed whether the dynamics were influenced by the type of anesthetic agent utilized in anesthetized recordings (**Figure 9E**). Neurons recorded under urethane anesthesia were the majority in type 1, 6, and 7. Moreover, these types lacked neurons recorded under isoflurane. Similarly, there were no isoflurane neurons in type 3, but this type contained a higher proportion of chloral hydrate neurons. Finally, type 2 and 4 contained neurons recorded under isoflurane, as well as those recorded under chloral hydrate, in greater proportions. Thus, we found 75% of the second-order spike train patterns identified differed in their composition of neurons recorded under urethane, chloral hydrate, and/or isoflurane.

Specific disease models and genetic modifications were associated with different second-order spike train dynamics

Finally, we tested whether genetic manipulations for opto/chemo-genetics (Cre-expression) and models of neurodegenerative disease (i.e., genetic modification or pharmacological manipulations) were over- or under-expressed in any of the return map types (**Figure 9F-G**). We found that type 2 had an increased proportion of neurons from pharmacological animal models of dyskinesia and Parkinson's disease, but a decreased proportion of neurons from APP/PS1 genetic model and DSP-4 pharmacological model of neurodegenerative disease (**Figure 9F**). In contrast, we observed the opposite patterns in type 1 and 3. These clusters contained more APP/PS1 and DSP-4 neurons, but almost entirely lacked neurons from the pharmacological models of Parkinson's disease and dyskinetic disorders.

Lastly, we examined the representation of genetic manipulation for Cre expression across the 8 types of return density patterns (**Figure 9G**). We found type 2 was almost entirely comprised of wild-type animals. Type 3 had a higher proportion of TH-cre neurons, while type 5 and 8 had a greater proportion of neurons recorded DBH-cre animals. Although not a large difference, types 3, 5, and 8 also had an increased proportion of neurons from VGAT-cre animals. These results show that TH-cre, DBH-cre, and VGAT-cre expressing neurons may each be biased toward specific relative firing patterns. Importantly, however, one type of firing pattern (type 2) was expressed only in wild type subjects.

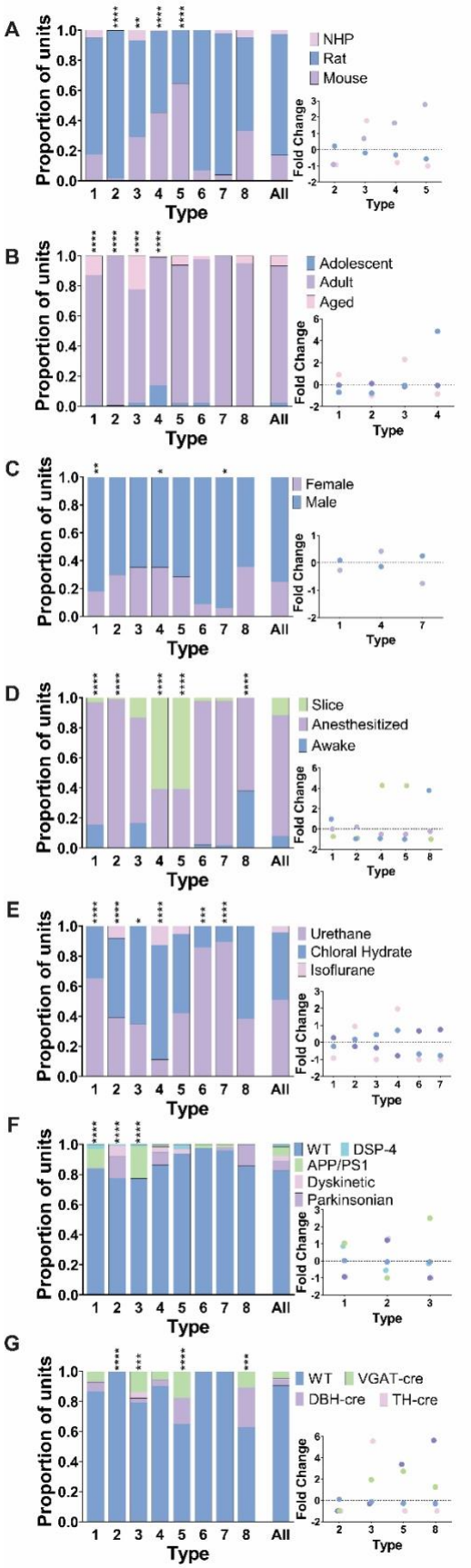

Figure 9: Age, state, and other factors contribute to unique second order spike train dynamics. Bar graphs show the proportion of traits represented in each of the 8 return density types (type ID on x axis) and the population as a whole (rightmost bar). The proportion of traits in each cluster is identified in each bar graph and was tested for differences compared to the overall population with a chi-squared test. Fold change in proportional representation is shown in the bottom right insert for types where there was a significantly different proportion of traits. Fold change was calculated as (trait proportion within type-proportion in population)/proportion in population). **A)** Four types were comprised of neurons across species in different proportions compared to the population. Type 2 contained almost entirely neurons from rats while there was an overrepresentation of mouse neurons in type 4 and 5. Nonhuman primate neurons were overrepresented in type 3 return density plots. **B)** Age impacted the types of return density plots LC neurons fell into. Types 1-4 were comprised of significantly different proportions of neurons based on age. There was an increase in adolescent neurons in type 4, adult neurons in type 2, and aged neurons in types 1 and 3. **C)** Three of the return density types (1,4, and 7) contained different proportions of neurons from males and females. **D)** State varied greatly across the 8 second order types. Types 4 and 5 have more neurons from reduced preparations, 1 and 8 had more neurons from awake animals, and type 2 is almost all from anesthetized neurons. **E)** Almost all types had different proportions of anesthesia types compared to the overall population of neurons. **F)** Disease model representation differed in types 1, 2, and 3. There is an overrepresentation of APP/PS1 and DSP-4 neurons in types 1 and 3 and an overrepresentation of parkinsonian and dyskinetic pharmacological models in type 2. **G)** Types 3, 5, and 8 contained increased proportions of neurons from genetically manipulated animals while type 2 was almost entirely from wild type animals.

Discussion

The LC is an ancestral brain region whose form and function has been conserved across species including fish, amphibians, reptiles, and mammals. We hypothesized that LC activity (spike rate and firing patterns) would be largely identical across species. We furthermore hypothesized that the activity of an evolutionarily ancient brain region would be affected similarly by sex, age, and experimental preparation or brain state across species. By analogy: breathing in mammals, whether the individuals are male or female – young or old – asleep or awake – is driven by homologous brainstem (pre-Bötzinger nucleus) activity patterns regardless of these biological factors. At first glance, this would appear true for LC neurons which tend to fire around 1 spike/sec and exhibit two firing modes (phasic or tonic) in vertebrates. However, the hypothesis we propose has never been tested due to the low sample sizes used in individual studies. By pooling data and using a powerful binomial regression model, we show that LC firing rates vary due to a complex interplay between species, sex, age, and brain state. In short, LC activity – and its relationship with core biological factors – is not conserved across species. In fact, the differences in firing rate (0.12 to 3.1 spikes/sec) represent relatively large deviations in neuronal activation given the low level of spontaneous LC activity (around 1 spike/sec).

LC firing rate and firing patterns are associated with complex interaction between species and biological factors

Although, in principle, the firing rate of LC neurons appears to be similar between fish, mice, rats, and NHPs in datasets collected over decades of individual studies (Vreven et al., 2024), a direct comparison has not been made on single large dataset with a model controlling for individual and combined effects. We found that the firing rate in mice is elevated compared to rats and NHPs. We also observed that specific fast, rhythmic and fast, semi-rhythmic firing patterns, as well as single attractor dynamics (Poincaré plots type 4 and 5) were enriched with neurons recorded in mice. Male mice have become a predominant species in research due to their accessibility for genetic modification. Intriguingly, we found that brain-wide genetic manipulation not directly focused on the LC may affect both firing rate (VGAT-cre mice) and temporal spiking patterns (VGAT-cre and DBH-cre mice). One caveat, however, is that most of the genetic manipulation data were collected by a single laboratory and should therefore be assessed across laboratories before drawing firm conclusions.

We found that species differences in neuronal activity interact with biological factors, such as sex and brain state. For instance, in mice, activity was generally higher under anesthesia and in brain slices and lower during wakefulness, whereas in rats the opposite pattern was observed (we did not have NHP data from different experimental preparations for comparison). Neurons recorded from female rats were more active than those recorded from male rats or NHP, whereas in mice, female LC neurons are less active than male during awake states but more active in brain slice preparations. While it is known that the LC is a sexually dimorphic structure (Pinos et al., 2001; Bangasser et al., 2011; Bangasser et al., 2016; Mariscal et al., 2023), a direct comparison of LC activity between sexes has not been performed on a large scale. Our findings may implicate the increased activity of female LC as a driver of sex-specific vulnerability to stress, anxiety, and substance-use disorder (Brady and Randall, 1999; Altemus et al., 2014; Bangasser and Valentino, 2014; Bangasser et al., 2016). Critically, however, our analysis identifies potential mechanistic differences in the neural circuits underlying sex-related stress and anxiety across species that may impact translatable findings.

Do LC neurons spontaneously burst, and are bursts the same across species?

We saw evidence of spontaneous bursting from LC neurons (without evoked triggers) and investigated whether LC bursts are fundamentally the same across species and biological factors. We observed a diverse collection of ISI histogram distributions that fell into 17 different neuronal clusters. These clusters could be roughly grouped into 3 types of firing pattern: *(i)* fast and rhythmic (rare), *(ii)* fast and semi-rhythmic (frequent), or *(iii)* irregular (most common). Each of these three qualitative firing pattern groups contain numerous patterns differentiated, for example, by the peak ISI time of the neurons in that cluster. Although distinct ISI cluster groups varied between different experimental parameters, each broad pattern

group was found across multiple sex, species and experimental preparations. Overall, this indicates abundant heterogeneity within the characteristics of spontaneous bursting by LC neurons.

We assessed the second-order temporal dynamics of LC activity using Poincaré plots to look at the temporal organization of ISIs among individual LC neurons (Siegel, 1990; Carlson and Foote, 1992; Szücs et al., 2005). We observed 8 pattern types, which could be coarsely grouped into either single attractor or multi-attractor dynamics in the spike train. Single attractor dynamics are characterized by a temporally-stable and repetitive pattern of spiking with varying levels of regularity, while multi-attractor dynamics meant that neurons switched between stable attractors of specific firing patterns that could be bursts, semi-regular activity, or irregular activity.

Our findings suggest that the classical conceptual two-mode model of LC neuronal activity may be a somewhat impoverished view. The irregular firing patterns that emerged from this large dataset are consistent with the “tonic” firing mode, which has been defined as spontaneous spiking (~ 0.1 to 5 spikes/sec) with long, and variable ISIs (Foote et al., 1980). However, it is apparent from the ISI histograms and the Poincaré plots that there is substantial diversity in individual tonic baseline range and regularity of firing. This diversity in tonic activity is driven by species differences, age and experimental preparation. Phasic burst firing in LC neurons has multiple definitions in the literature, including simply a transient elevation due to spontaneous (internally-driven) or sensory evoked firing rate (Aston-Jones and Bloom, 1981b; Aston-Jones et al., 1994; Marzo et al., 2014; Neves et al., 2018), or a burst of successive spikes with an ISI of less than 80 msec (Tung et al., 1989; Saunier et al., 1993; Nilsson et al., 2005; Miguelez et al., 2011a; Cieslak et al., 2017; Liu et al., 2017). Here, we show that rhythmic burst firing occurs frequently in several species and is expressed over a broad range of potential patterns across LC neurons. Overall, this result suggests that LC neuronal activity patterns are heterogeneous and diverse.

The LC dual-mode of operation has been widely used outside of neurophysiology. For instance, human neuroimaging studies and cognitive psychology studies invoke the dual-mode conceptual framework to link pupillometry measurements with cognitive processes (Coull, 1998; Einhauser et al., 2008; Murphy et al., 2011; Alnaes et al., 2014; Murphy et al., 2014; van den Brink et al., 2016a; van den Brink et al., 2016b; Elman et al., 2017; He et al., 2020). The broadening of LC modes of operation may have importance for human subjects research that uses pupillometry.

The heterogeneity of LC firing patterns has important implications for experiments probing LC function through optogenetic or electrical stimulation, which drive neurons at a specific timing and pattern (Carter et al., 2010; Marzo et al., 2014; Vazey et al., 2018; Harley and Yuan, 2021; Grimm et al., 2024). Stimulation parameters for these studies are consistently applied and do not reflect the underlying

population heterogeneity and "multi-mode" model of LC activity revealed by this data-driven, large dataset approach. This diversity in LC activity patterns also has implications for understanding neuromodulation across species and different biological factors. For instance, when rodent LC neurons emit spikes at a short ISI, their axons can become depolarized so that subsequent spikes in the burst are conducted faster (Aston-Jones et al., 1980). Indeed, this may explain findings from studies in rodents showing that, in contrast to periods in which LC activity is tonically elevated, a transient burst can increase the magnitude of NE release (Florin-Lechner et al., 1996; Devoto et al., 2005b). Bursts differentially release co-transmitters, and LC neurons release numerous neuropeptides such as galanin, neuropeptide Y, and brain derived neurotrophic factor, as well as other small molecule neurotransmitters such as dopamine, glutamate, and ATP (Castren et al., 1995; Conner et al., 1997; Simpson et al., 1999; Devoto et al., 2001; Poelchen et al., 2001; Devoto et al., 2005a; Schwarz and Luo, 2015; Takeuchi et al., 2016; Yang et al., 2021). The differential expression of diverse firing patterns across species and biological factors suggests that the neurotransmitter release properties and functional effects of LC neurons could have nuanced and previously unappreciated differences based on species, sex, age, and brain state.

Brain slices and anesthesia provide a window into the pacemaker dynamics of LC activity

Experiment preparations, such as anesthetized recordings and *ex vivo* brain slice recordings, matched awake firing rate quite closely (although there was the notable interaction with both species and sex). On the other hand, brain slices were primarily associated with distinct firing patterns (ISI histograms) and spike timing dynamics (Poincaré plots).

Brain slice recordings were strongly associated with pacemaker-like, rhythmic spike patterns with low ISI variability, while awake or anesthetized preparations had more variable, semi-rhythmic or irregular firing patterns. Neurons recorded *ex vivo* were more likely to be found in type 4 and type 5 Poincaré plots, which had the smallest amount of variability. This contrast in activity may be explained by the severance of afferent connections and removed external sensory input which affects both anesthetized and awake LC activity (Aston-Jones and Bloom, 1981b; Sara and Bouret, 2012).

While pacemaker-like activity was most prominent in brain slices, such patterns were still observed in anesthetized and awake animals. Thus, such patterns of firing are not "artifacts" or "unnatural" brain activity, rather they are the reality of the preparation being used. In other words, the LC has a range of firing patterns that are apparent in all experimental preparations, but some preparations emphasize particular patterns over others and are thus a good experimental preparation for studying those situations.

It is useful to understand the role of LC pacemaker activity in awake animals and brain slices may be an ideal system to study this phenomenon. Moreover, emerging *in vitro* models of LC organoids that

incorporate human pluripotent stem cells may be a useful method for understanding how human LC development and gene expression affect LC pacemaker activity (Tao et al., 2023).

LC firing is affected in aging and neurodegenerative disorders

We found that LC firing gradually increased with age, consistent with some recent human imaging data (Ludwig et al., 2024) and a recent mouse slice recording study (Budygin et al., 2024). To our knowledge, prior studies assessing age-related changes in LC activity in anesthetized rats observed either no differences, or a decrease with age (Olpe and Steinmann, 1982). This discrepancy may be due to the age ranges, smaller sample sizes, or brief duration of recordings (3 min) used in the prior work (recordings in this large dataset ranged from ~5 seconds to ~7 hours with a median of 444 seconds). We also observed semi-rhythmic firing in the adolescent LC that becomes predominantly irregular in adulthood and finally transitions into more rhythmic, faster activity in aged animals. One reason for late stage reversion to rhythmic firing patterns and increased firing rates could be compensation for NE fiber loss as a natural course of aging, which has been observed in both aging rodents and humans (Rorabaugh et al., 2017; Chalermpalanupap et al., 2018; Kelberman et al., 2022; Langley et al., 2022). Interestingly, age-related changes appear to be shared across the three species tested in this study. Age-related changes may be important for understanding how the immune system, metabolism, cardiac function, cognitive abilities, and behavior (which are all influenced by LC activity) change as organisms grow older.

The LC and its dysfunction have long been implicated in neurodegenerative disorders (Mann et al., 1980; van Dongen, 1981; Sturrock and Rao, 1985b; German et al., 1992; Mather and Harley, 2016; Weinshenker, 2018; Liu et al., 2020). Surprisingly, most disease models were not associated with altered spike rate. This is unexpected given prior work showing differences for the APP/PS1 model (Kelberman et al., 2023; Kelly et al., 2021.) In slice recordings, LC neurons from APP-PSEN1 male mice were more spontaneously active than wild-type controls (Kelly et al., 2021). On the other hand, extracellular LC recordings (chloral hydrate anesthesia) from male and female APP/PS1 rats (Fischer background) were less active than wild-type rats (Kelberman et al., 2023). The opposing findings in prior work may be due to the phenotypic differences between the rats and mice despite having the same genetic mutation. For instance, the APP/PS1 rat develops LC tau pathology, whereas the APP-PSEN1 mice only accumulate Aβ oligomers in the LC (Rorabaugh et al., 2017; Kelly et al., 2021). Unexpectedly, our analysis revealed no difference in LC firing rate between animals with the APP/PS1 genetic mutation and wild-type controls. However, our analysis compared to wild-type neurons from NHPs, rats, and mice under a variety of conditions (sex, age, experimental preparation). Our work shows that other factors influence LC activity, and it is noteworthy that the prior assessment of the APP/PS1 model in rats used an extracellular recording preparation and older animals (6 and 15 months) compared to the recordings in mice, which

were in slice and at an earlier age (2 to 4 months). The null finding in our large-scale study does not necessarily suggest that individual studies are incorrect. Instead, our report highlights that disease-related genetic modifications likely require the most stringent controls (i.e., using littermates of same age, sex, background, rearing conditions, recording preparation, etc.) to make a comparison with the wild-type control group. The need for careful controls is all-the-more relevant when considering that the effects of a mutation may be of small magnitude (less than 1 spike/sec) and sample sizes are typically many magnitudes smaller than the large dataset analyzed in the present study.

One point of consensus with prior work on the APP/PS1 genetically-modified rat is that the LC neurons display abnormal bursting characteristics (Kelberman et al., 2023). Similarly, we found that APP/PS1 neurons fired in a short ISI pattern. Temporal firing patterns appeared to discriminate other genetic modifications and neurodegenerative disease models, as well. APP/PS1 (and DSP-4) animals are overrepresented in type 1 and type 3 Poincaré plots and underrepresented in type 2 Poincaré plots, whereas dyskinetic and parkinsonian rat models had the opposite patterns. The common feature is that these patterns are all single attractors. Thus, temporal dynamics of LC firing may be more informative of LC neuronal dysfunction in neurodegenerative disorders than population level firing rates.

Integration of the ancestral LC into vertebrate nervous systems may be a bespoke solution for some species

Using the shared contributions of data from multiple laboratories, our analysis uncovered specific differences in firing rate and firing patterns that also depended on biological factors such as sex and age. Although the LC is an ancestral brain region shared by vertebrates, its activity and functions have not been tightly conserved. The LC likely integrated into vertebrate nervous systems within the variable context of the evolutionary pressures that sculpted the nervous system of each species. Via its broad central nervous system-wide connectivity, this ancestral region may contribute to sex, species, and age-related differences in cognition, behavior, cardiovascular function, the immune system, and metabolism. A deeper understanding of how the LC is functionally integrated in the nervous system across a range of species may help explain the relationship that sex and age have with psychiatric, cardiovascular, immunological, and metabolic disease.

Methods

Ethical guidelines. All animal studies in the United States were performed with approval from the Institution Animal Care and Use Committee at Baylor College of Medicine, Cold Spring Harbor, Columbia University, Emory University, Massachusetts Institute of Technology, New York University, Rowan University, University of North Carolina Chapel Hill, University of Pennsylvania, University of Wisconsin-Madison, Washington University School of Medicine, University, and Yale University in accordance with the National Institutes of Health Guide for the Care and Use of Laboratory Animals. Approval for animal studies outside of the United States were approved by the Animal Care and Experimentation Committee of the Institute for Research in Fundamental Sciences, the Animal Care and Use Committees of the RIKEN Brain Science Institute, the Institutional Animal Care and Use Committee of National Taiwan University, the Institutional Animal Care and Use Committee of Chung-Shan Medical University, the University of Bristol Animal Welfare and Ethical review body according to the UK Animals (Scientific Procedures) Act 1986 (license PPL3003362), the Committee for Animal Experimentation at the University of Cadiz and University of the Basque Country (UPV/EHU), in compliance with the European Community Guidelines for the Care and Use of Laboratory Animals (2010/63/EU) and Spanish Law for the protection of animals used for research experimentation and other scientific purposes (RD 53/2013), the Committee for Animal Experimentation at the University of Cadiz, The Regierungspräsidium Tuebingen & The Regional State Administrative Agency for Southern Finland according to German Law for the Protection of Animals in experimental research (Tierschutzversuchstierverordnung) & the European Community Guidelines for the Care and Use of Laboratory Animals (EU Directive 2010/63/EU).

Data Collection and Organization

Data was sourced from various labs and imported into a custom structure in Matlab (MathWorks; version R2019a) for analysis. We acquired data on species, sex, strain, state (awake, slice, anesthesia and type), age, pharmacology and events (type and timestamp), and genotype. LC recordings were imported as timestamps of each individual spike within a given recording. Firing rates were calculated as the number of spikes divided by the timestamp of the last recorded spike.

Data Curation

A total of 2944 neurons were submitted across 20 labs. After excluding 975 neurons as mentioned in **Figure 1** (ISI violation n=319, recording length violation n=457, stress n=199) the resulting

1969 neurons were further curated for firing rate analysis and interspike interval analysis separately. Firing rate analysis further excluded 113 neurons where the sex was unknown and 1 single neuron recorded under pentobarbital anesthesia for a final dataset of 1855 neurons. Interspike interval dataset included neurons from animals of unknown sex but excluded units that did not have at least 100 interspike intervals prior to any stimulus or pharmacology application (n=260). This exclusion criteria resulted in a total of 1708 single neurons included for ISI analysis.

Statistical analysis of firing rates

Descriptive statistics were used to describe the characteristics of the sample of firing rates. Given the multitude of variables present in our analyses, we fit a regression to explain the individual and combined effects of factors on firing rates. Initial examination of the data revealed overdispersion. We therefore chose a negative binomial regression model, which is commonly used to model overdispersed data. Negative binomial regression is a generalization of a Poisson regression with less restrictive assumptions of equal mean and variance which was also present in our data. Given that we wanted to leverage cross-lab comparisons, we removed lab as a random effect and fit a marginal model instead. This was further justified by the large size of our dataset and model fit statistics (ratio of the deviance to degrees of freedom and dispersion parameter). A generalized estimating equation algorithm was then used to estimate the independent effects of individual factors and their interactions on firing rates (SAS PROC GENMOD).

Generalized estimating equations (GEE) are one popular algorithm for fitting marginal models when outcome is a discrete variable. Using GEE with offset of measurement time, the independent effect of age, sex, species, genotype and anesthesia/state as well as their effect modification on firing rate were assessed. If a significant effect modification (interaction) was present, estimated firing rate was compared at a different level of the components of the interaction. If the interaction was not significant, estimated firing rate was reported with adjustment of other features. GEE was also applied to the comparison of firing rate between single or various combination of methods which were used to verify locus coeruleus neurons. To correct for multiple comparisons, a false-discovery rate of < 20% was applied and Benjamini-Hochberg procedure was used. All analyses were performed in SAS® 9.4 (SAS Institute Inc). All tests performed were two-tailed.

Data Visualization

Data are visualized by plotting individual data points with a box representing the estimated mean firing rate ± 95% confidence interval on a log10 scale. Effect size plots include the difference between the estimated means ± 95% confidence interval. Graphs were made in GraphPad Prism (version 9.2.0).

ISI

For each neuron, spiketimes from the beginning of the recording until administration of pharmacology, any event timestamps, or the end of the recording (whichever was first) were used to calculate ISIs. ISIs were calculated by subtracting the time of each spike from the following spike time ($spike_{x+1}$-$spike_x$), resulting in a train of ISIs for each neuron. The mean value for all ISIs was 1.096s ± 17.573s SD.

Principal components analysis

To identify patterns in ISI distributions across neurons, ISI histograms (20ms bins, 0 to 2.5s, normalized) were analyzed using PCA. Principal component 1 explained 27.43% of variance and PC2, PC3, PC4, PC5, and PC6 explained 17.31%, 11.53%, 7.43%, 6.08%, and 4.88% respectively (**Supplemental Figure 2**). In total the first 6 principal components explain 74.67% of variance. Clustering was performed on the first 6 principal components using the Matlab kmeans function. Using a gap test, the optimal number of clusters was identified as 17 using squared euclidean distance.

Grouping ISI clusters

After neurons were clustered based on ISI distributions, we further grouped the 17 clusters based on the peak ISI time and kurtosis of ISI distribution. Kurtosis is a measure of the 'tailedness' of a distribution, or how often an observation in a distribution falls in the center, where a high kurtosis value means low tailedness or most observations falling in the peak. The kurtosis of each cluster was identified by finding the kurtosis of the average ISI distribution of all neurons in a cluster using Graphpad Prism. The ISI most likely to occur for each cluster was identified by the time bin with the highest probability from the mean ISI histograms of all neurons in a cluster. Kurtosis was compared to the maximum probability ISI for each cluster. Graphing these characteristics for each cluster identified 3 main groups of clusters (**Figure 6B**).

Return Density plots

Second order ISI patterns were characterized using return density plots to visualize unique temporal patterns of single units. These return density plots show the ISI of a single neuron on the x axis plotted against the following ISI of that same neuron on the y axis. A two-dimensional histogram was created for each unit (ISI_n x ISIn+1) binned in 40 bins on each axis centered around the maximum value in the two-dimensional histogram (±5) plotted on a logarithmic scale for better visualization. Areas with colors approaching yellow indicate a higher density, or likelihood, where cooler colors indicate lower density and zero density areas are colored blue. Example return density plot and raster plots are shown in Figure 8A-B to demonstrate how neural data is represented.

We identified unique patterns in the return density plots of single units and grouped the units based on these patterns. We visually identified 8 temporal patterns ('types 1-8') and manually curated the return density plots into each type. When sorting units into types the return density plots were aligned to show the max bin in the center of the return density plot and neurons were assigned into types based on their shape and not the values on the x and y axis.

Trait comparisons across ISI groupings

To identify if clusters (histograms) or types (return density plots) were comprised of more/less neurons with certain traits, we compared the proportion of a given trait within each cluster/type to the overall population of neurons in the dataset. The proportion of neurons containing certain traits in each cluster/type (for both PCA clustered ISI distributions and return density plot types) were compared to identify if any given trait was more likely to result in a specific activity pattern. Characteristics examined included species, sex, age, state, anesthesia type, disease model and genotype. Differences in the frequency of a given trait (ex. male vs female) in each cluster were compared to the frequency of these traits in the population of neurons included in ISI analysis using the chi-squared test with Bonferroni correction for multiple comparisons.

Supplemental Figures

Supplemental Figure 1: Effect of species and state interaction on LC firing rates under A) urethane and B) isoflurane anesthesia.

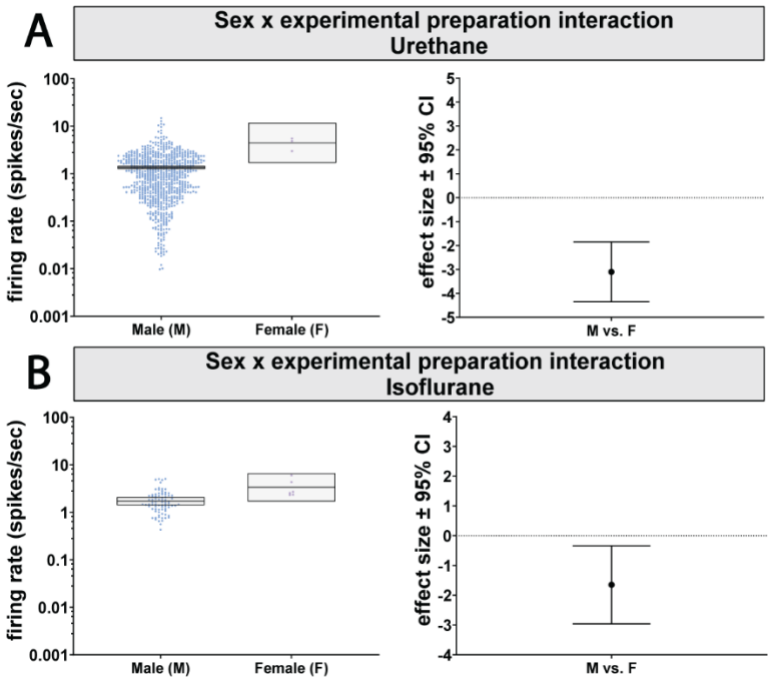

Supplemental Figure 2: Variance explained in ISI distribution PCA.

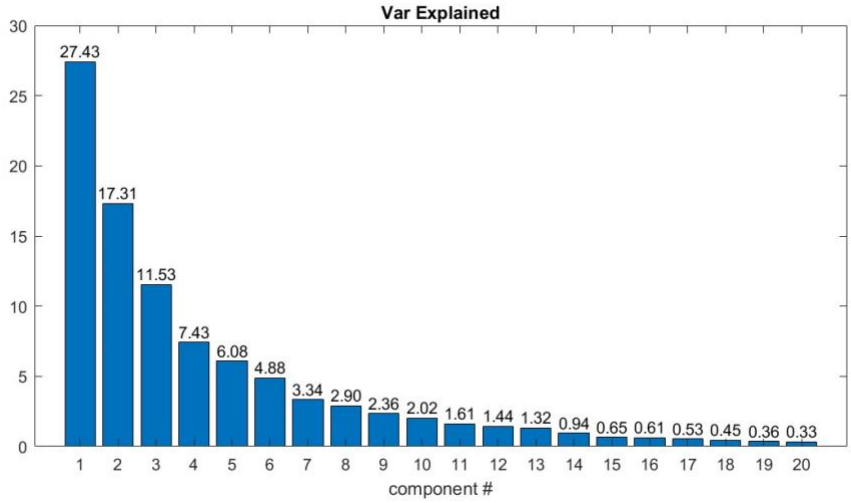

Supplemental Table 1A: Estimated Firing Rates Based on Main Effects of Individual Factors

Factor	**Sub-Factor**	**DF**	**Chi-Square (Wald Test)**	**Estimated Firing Rate** **Mean ± SEM (95% CI)**	**Main Effect (p-value)**
Age	Adolescent	2	10.34	1.17 ± 0.10 (0.99 - 1.38)	0.0057
	Adult			1.57 ± 0.03 (1.50 - 1.63)	
	Aged			1.86 ± 0.13 (1.61 - 2.14)	
Sex	Male	1	12.98	1.47 ± 0.03 (1.41 - 1.54)	0.0003
	Female			1.87 ± 0.07 (1.73 - 2.02)	
Species	Mouse	2	42.61	2.27 ± 0.13 (2.03 - 2.53)	<0.0001
	Rat			1.48 ± 0.03 (1.42 - 1.54)	
	NHP			1.41 ± 0.19 (1.09 - 1.83)	
Genotype/Disease Models	Wild-type	7	69.75	1.55 ± 0.03 (1.48 - 1.62)	<0.0001
	DBH-cre			2.15 ± 0.44 (1.44 - 3.21)	
	TH-cre			2.23 ± 0.42 (1.54 - 3.22)	
	VGAT-cre			1.04 ± 0.15 (0.79 - 1.37)	
	APP/PS1			1.50 ± 0.12 (1.28 - 1.74)	

	DSP-4			2.35 ± 0.36 (1.75 - 3.17)	
	Dyskinetic			1.84 ± 0.22 (1.45 - 2.33)	
	Parkinsonian			1.51 ± 0.12 (1.29 - 1.77)	
State/Anesthesia	Awake	4	33.33	1.45 ± 0.14 (1.20 - 1.76)	<0.0001
	Slice			1.67 ± 0.09 (1.50 - 1.86)	
	Chloral Hydrate			1.73 ± 0.05 (1.63 - 1.84)	
	Urethane			1.37 ± 0.04 (1.28 - 1.45)	
	Isoflurane			1.84 ± 0.17 (1.54 - 2.20)	

Supplemental Table 1B: Summary of Interactions between Factors on Firing Rates

Interaction	**DF**	**Chi-Square (Likelihood Ratio Test)**	**p value**
Age*Sex	2	3.82	0.15
Age*Species	-	-	Non-estimable
Age*Genotype	1	0	0.97
Age*Anesthesia	-	-	Non-estimable
Sex*Species	1	6.59	0.0103

Sex*Genotype	5	6.24	0.28
Sex*Anesthesia	3	13.12	0.0044
Species*Genotype	-	-	Non-estimable
Species*Anesthesia	3	15.7	0.0013
Genotype*Anesthesia	-	-	Non-estimable

Supplemental Table 2: Post-hoc Pairwise Comparisons of Firing Rates Based on Main Effect of State

Comparison	DF	Chi-Square (Wald Test)	Effect Size (95% CI)	p-value
Awake ***vs*** Chloral Hydrate	1	3.376	-0.28 (-0.60 – 0.04)	0.07
Awake ***vs*** Isoflurane	1	3.116	-0.39 (-083 – 0.05)	0.08
Awake ***vs*** Slice	1	1.705	-0.22 (-0.57 – 0.13)	0.19
Awake ***vs*** Urethane	1	0.352	0.08 (-0.18 – 0.34)	0.55
Chloral Hydrate ***vs*** Isoflurane	1	0.385	-0.11 (-0.42 – 0.20)	0.53
Chloral Hydrate ***vs*** Slice	1	0.281	0.06 (-0.14 – 0.26)	0.60
Chloral Hydrate ***vs*** Urethane	1	27.743	0.36 (0.23 – 0.49)	<0.0001
Isoflurane ***vs*** Slice	1	0.756	0.17 (-0.24 – 0.47)	0.38
Isoflurane ***vs*** Urethane	1	7.482	0.47 (0.21 - 0.73)	0.0062
Slice ***vs*** Urethane	1	9.037	0.30 (0.13 – 0.47)	0.0026

Supplemental Table 3A: Post-hoc Pairwise Comparisons of Firing Rates Based on the Interaction between State and Sex, Males

Contrast	DF	Chi-Square (Wald Test)	Effect Size (95% CI)	p-value
Awake ***vs*** Chloral Hydrate	1	0.02	0.03 (0.33 – 0.39)	0.89
Awake ***vs*** Isoflurane	1	0.13	-0.09 (-0.57 – 0.30)	0.71
Awake ***vs*** Slice	1	0.37	0.12 (-0.26 – 0.51)	0.54
Awake ***vs*** Urethane	1	2.47	0.29 (0 – 0.58)	0.12
Chloral Hydrate ***vs*** Isoflurane	1	0.41	-0.12 (-0.45 – 0.21)	0.52
Chloral Hydrate ***vs*** Slice	1	0.61	0.09 (-0.16 – 0.34)	0.43
Chloral Hydrate ***vs*** Urethane	1	9.65	0.26 (0.11 – 0.41)	0.0019
Isoflurane ***vs*** Slice	1	1.21	0.21 (-0.15 – 0.57)	0.27
Isoflurane ***vs*** Urethane	1	4.92	0.37 (0.12 – 0.64)	0.0266
Slice ***vs*** Urethane	1	2.084	0.17 (-0.02 – 0.36)	0.15

Supplemental Table 3B: Post-hoc Pairwise Comparisons of Firing Rates Based on the Interaction between State and Sex, Females

contrast	DF	Chi-Square (Wald Test)	Effect Size (95% CI)	p-value
Awake ***vs*** Chloral Hydrate	1	21.11	-0.96 (-1.74 – -0.18)	<0.0001
Awake ***vs*** Isoflurane	1	4.49	-2.49 (-4.10 – -0.88)	0.0341
Awake ***vs*** Slice	1	17.08	-1.11 (-2.00 – -0.22)	<0.0001
Awake ***vs*** Urethane	1	2.65	-3.56 (-5.57 – -1.55)	0.10
Chloral Hydrate ***vs*** Isoflurane	1	1.73	-1.53 (-2.79 – -0.27)	0.19
Chloral Hydrate ***vs*** Slice	1	0.57	-0.16 (-1.38 – 1.08)	0.45
Chloral Hydrate ***vs*** Urethane	1	1.42	-2.60 (-4.37 – -0.83)	0.23
Isoflurane ***vs*** Slice	1	1.37	1.38 (-0.12 – 2.88)	0.24
Isoflurane ***vs*** Urethane	1	0.19	-1.07 (-6.32 – 4.18)	0.66

contrast	DF	Chi-Square (Wald Test)	Effect Size (95% CI)	p-value
Slice ***vs*** Urethane	1	1.25	-2.45 (-4.53 – -0.37)	0.26

Supplemental Table 3C: Post-hoc Pairwise Comparisons of Firing Rates Based on the Interaction between State and Species, Rats

contrast	DF	Chi-Square (Wald Test)	Effect Size (95% CI)	p-value
Awake ***vs*** Chloral Hydrate	1	1.679	0.55 (-0.03 – 1.13)	0.20
Awake ***vs*** Isoflurane	1	2.030	0.64 (-0.10 – 1.38)	0.15
Awake ***vs*** Slice	1	5.523	1.01 (0.43 – 1.59)	0.0188
Awake ***vs*** Urethane	1	4.486	0.89 (0.40 – 1.38)	0.0342
Chloral Hydrate ***vs*** Isoflurane	1	0.291	0.09 (-0.23 – 0.41)	0.59
Chloral Hydrate ***vs*** Slice	1	17.046	0.46 (0.21 – 0.71)	<0.0001
Chloral Hydrate ***vs*** Urethane	1	24.686	0.34 (0.22 – 0.46)	<0.0001
Isoflurane ***vs*** Slice	1	3.778	0.37 (0.02 – 0.72)	0.05
Isoflurane ***vs*** Urethane	1	2.209	0.25 (-0.-2 – 0.52)	0.14
Slice ***vs*** Urethane	1	1.258	-0.12 (-0.33 – 0.09)	0.26

Supplemental Table 3D: Post-hoc Pairwise Comparisons of Firing Rates Based on the Interaction between State and Species, Mice

contrast	DF	Chi-Square (Wald Test)	Effect Size (95% CI)	p-value
Awake ***vs*** Chloral Hydrate	1	19.763	-1.35 (-2.36 – -0.34)	<0.0001
Awake ***vs*** Isoflurane	1	12.074	-2.17 (-3.57 – -0.77)	0.0005
Awake ***vs*** Slice	1	27.122	-1.33 (-2.30 – -0.36)	<0.0001

contrast	DF	Chi-Square (Wald Test)	Effect Size (95% CI)	p-value
Awake ***vs*** Urethane	1	10.478	-3.02 (-4.81 – -1.23)	0.0012
Chloral Hydrate ***vs*** Isoflurane	1	1.637	-0.82 (-1.90 – 0.26)	0.20
Chloral Hydrate ***vs*** Slice	1	0.004	0.02 (-0.56 – 0.60)	0.95
Chloral Hydrate ***vs*** Urethane	1	3.129	-1.67 (-3.00 – -0.34)	0.08
Isoflurane ***vs*** Slice	1	1.831	0.84 (-0.13 – 1.81)	0.18
Isoflurane ***vs*** Urethane	1	0.609	-0.85 (-2.96 – 1.26)	0.44
Slice ***vs*** Urethane	1	3.297	-1.69 (-2.87 – -0.51)	0.07

Supplemental Table 4: Post-hoc Pairwise Comparisons of Firing Rates Based on Main Effect of Sex

Comparison	DF	Chi-Square (Wald Test)	Effect Size (95% CI)	p-value
Male ***vs*** Female	1	24.61	-0.40 (-0.53 – -0.27)	<0.0001

Supplemental Table 5A: Post-hoc Pairwise Comparisons of Firing Rates Based on the Interaction between Sex and State, Male vs Female

Contrast (Male vs. Female)	DF	Chi-Square (Wald Test)	Effect Size (95% CI)	p-value
Awake	1	8.309	0.75 (0.00 – 1.50)	0.0039
Chloral Hydrate	1	4.617	-0.24 (-0.45 – -0.03)	0.0317
Isoflurane	1	1.988	-1.65 (-2.96 – -0.34)	0.16
Slice	1	5.105	-0.48 (-0.86 – -0.09)	0.0239
Urethane	1	2.015	-3.1 (-4.35 – -1.85)	0.16

Supplemental Table 5B: Post-hoc Pairwise Comparisons of Firing Rates Based on the Interaction between Species and Sex, Rats

Contrast	DF	Chi-Square (Wald Test)	Effect Size (95% CI)	p-value
Male vs Female	1	26.76	-0.45 (-0.59 – -0.31)	<0.0001

Supplemental Table 5C: Post-hoc Pairwise Comparisons of Firing Rates Based on the Interaction between Species and Sex, Mice

Contrast	DF	Chi-Square (Wald Test)	Effect Size (95% CI)	p-value
Male vs Female	1	4.49	0.52 (0.02 – 1.02)	0.034

Supplemental Table 6: Post-hoc Pairwise Comparisons of Firing Rates Based on Main Effect of Species

Comparison	DF	Chi-Square (Wald Test)	Effect Size (95% CI)	p-value
Rat ***vs*** Mouse	1	36.537	-0.79 (-0.97 – -0.61)	<0.0001
NHP ***vs*** Mouse	1	14.450	-0.86 (-1.49 – -0.23)	0.0001
Rat ***vs*** NHP	1	0.135	0.07 (-0.44 – 0.30)	0.71

Supplemental Table 7A: Post-hoc Pairwise Comparisons of Firing Rates Based on the Interaction between Species and State, Mice vs. Rats vs. NHPs

	Effect Size (95% CI)			p-value (DF, Chi-Square [Wald Test])		
Anesthesia	Rat ***vs*** Mouse	NHP ***vs*** Mouse	Rat ***vs*** NHP	Rat ***vs*** Mouse	NHP ***vs*** Mouse	Rat ***vs*** NHP
Awake	1.34 (0.30 – 2.38)	0.52 (-0.15 – 1.19)	0.82 (0.02 – 1.61)	0.0036 (1, 8.472)	0.0491 (1, 3.871)	0.08 (1, 3.167)
Chloral Hydrate	-0.56 (-0.91 – -0.21)	-	-	0.0206 (1, 5.361)	-	-
Isoflurane	-1.47 (-2.33 – -0.61)	-	-	0.0170 (1, 5.697)	-	-
Slice	-1.00 (-1.49 – -0.60)	-	-	<0.0001 (1, 26.456)	-	-
Urethane	-2.57 (-3.20 – -1.94)	-	-	0.0049 (1, 7.913)	-	-

Supplemental Table 7B: Post-hoc Pairwise Comparisons of Firing Rates Based on the Interaction between Species and Sex (Males)

Contrast	DF	Chi-Square (Wald Test)	Effect Size (95% CI)	P value
Rat ***vs*** Mouse	1	35.57	-1.09 (-1.30 – -0.88)	<0.0001
NHP ***vs*** Mouse	1	17.1	-1.07 (-1.78 – -0.36)	<0.0001
Rat ***vs*** NHP	1	0.02	-0.02 (-0.35 – 0.31)	0.89

Supplemental Table 7C: Post-hoc Pairwise Comparisons of Firing Rates Based on the Interaction between Species and Sex (Females)

Contrast	DF	Chi-Square (Wald Test)	Effect Size (95% CI)	P value
Rat ***vs*** Mouse	1	0.42	-0.12 (-0.47 – 0.23)	0.52

Supplemental Table 8: Post-hoc Pairwise Comparisons of Firing Rates Based on Main Effect of Genotype/Disease Model

Comparison	DF	Chi-Square (Wald Test)	Effect Size (95% CI)	p-value
WT ***vs*** DBH-Cre	1	1.846	-0.60 (-1.16 – -0.04)	0.17
WT ***vs*** TH-Cre	1	2.585	-0.68 (-1.19 – -0.17)	0.11
WT ***vs*** VGAT-Cre	1	11.376	0.51 (0.12 – 0.90)	0.0007
WT ***vs*** APP/PS1	1	0.192	0.05 (-0.17 – 0.27)	0.66
WT ***vs*** DSP-4	1	5.092	-0.80 (-1.22 – -0.38)	0.0249
WT ***vs*** Dyskinetic	1	1.678	-0.29 (-0.62 – 0.04)	0.20
WT ***vs*** Parkinsonian	1	0.089	0.04 (-0.19 – 0.27)	0.77

Supplemental Table 9: Post-hoc Pairwise Comparisons of Firing Rates Based on Main Effect of Age

Comparison	DF	Chi-Square (Wald Test)	Effect Size (95% CI)	p-value
Adolescent ***vs*** Adult	1	13.920	-0.40 (-0.65 – -0.15)	0.0002
Adolescent ***vs*** Aged	1	16.818	-0.69 (-1.04 – -0.34)	<0.0001
Adult ***vs*** Aged	1	4.471	-0.29 (-0.51 – -0.07)	0.0345

Supplemental Table 10: Characteristics of Clusters Identified based on ISI Distributions

	Cluster ID	Neurons N (%)	Kurtosis	Peak time (ms)
Fast, rhythmic	**1**	15 (0.88%)	58.39	150
	2	7 (0.41%)	55.63	110
	3	17 (1%)	35.98	50
	4	8 (0.47%)	33.83	120
Fast, semi-rhythmic	**5**	24 (1.41%)	20.8	230
	6	49 (2.87%)	19.76	40
	7	53 (3.1%)	15.83	80
	8	37 (2.17%)	12.61	170
	9	33 (1.93%)	11.04	320
	10	146 (8.55%)	6.227	100
	11	160 (9.37%)	3.573	210
Irregular	**12**	115 (6.73%)	1.517	500
	13	225 (13.17%)	0.706	170
	14	145 (8.49%)	0.5535	760
	15	207 (12.12%)	0.5354	310
	16	178 (10.42%)	-1.084	490
	17	289 (16.92%)	-1.198	1050

Supplemental Table 11: Chi-Squared Tests on Trait Prevalence in ISI Distribution Clusters

	Species			Age			Sex			State			Anesthesia			Disease			Genotype		
Cluster ID	Chi-square	df	P value	Adjusted P value		Chi-square	df	P value	Adjusted P value		Chi-square	df	P value	Adjusted P value		Chi-square	df	P value	Adjusted P value		Chi-square	df	P value	Adjusted P value	
1	49.41	2	1.86E-11	3.17E-10	****	8.160	2	0.0169	0.2874		5.756	1	0.0164	0.2788		108.4	2	1E-15	1.7E-14	****	2.980	2	0.2277	1		3.153	4	0.5326	1		1.532	3	0.6749	1	
2	7.876	2	0.0196	0.331359		0.703	2	0.7035	1		0.051	1	0.8214	1		14.257	2	0.0008019	0.0136	*	3.908	2	0.1417	1		1.473	4	0.8314	1		0.715	3	0.8696	1	
3	4.107	2	0.1283	2.180533		13.62	2	0.0011	0.0188	*	2.381	1	0.1228	1		3.917	2	0.1410886	1		12.93	4	0.0116	0.1975		79.69	3	1E-15	1.7E-14	****
4	11.51	2	0.0032	0.053833		0.594	2	0.7431	1		0.229	1	0.6325	1		11.70	2	0.0029	0.0493	*	0.183	2	0.9126	1		1.460	4	0.8337	1		0.715	3	0.8696	1	
5	27.82	2	9.09E-07	1.55E-05	****	46.82	2	6.81E-11	1.16E-09	****	1.434	1	0.2312	1		124.9	2	1E-15	1.7E-14	****	0.3824	2	0.826	1		5.039	4	0.2834	1		2.449	3	0.4845	1	
6	4.874	2	0.0874	1.4858		54.197	2	1.703E-12	2.9E-11	****	7.535	1	0.0061	0.1037		3.449	2	0.1783	1		28.64	2	6.053E-07	1.03E-05	****	41.65	4	1.972E-08	3.35E-07	****	0.640	3	0.8872	1	
7	3.123	2	0.2098	3.567419		78.59	2	1E-15	1.7E-14	****	10.779	1	0.0010265	0.0175	*	7.461	2	0.023984	0.4077		15.28	2	0.00048	0.0082	**	10.03	4	0.04	0.68		7.702	3	0.0526	0.8942	
8	4.660	2	0.0969	1.628809		1.039	2	0.5949	1		1.853	1	0.1734	1		4.672	2	0.0967047	1		8.484	2	0.0144	0.2448		7.795	4	0.0994	1		2.145	3	0.5429	1	
9	36.37	2	1.26E-08	2.15E-07	****	89.87	2	1E-15	1.7E-14	****	1.013	1	0.3143	1		194.2	2	1E-15	1.7E-14	****	1.974	2	0.3726	1		6.283	4	0.1783	1		3.813	3	0.2823	1	
10	5.533	2	0.0629895	1.068782		56.22	2	6.21E-13	1.06E-11	****	2.817	1	0.0933	1		40.57	2	1.551E-09	2.64E-08	****	17.97	2	0.0001255	0.0021	**	71.38	4	1.2E-14	2.04E-13	****	23.98	3	2.521E-05	0.000429	***
11	17.142	2	0.0001895	0.003222	**	8.221	2	0.0164	0.2788		5.398	1	0.020155	0.3426		24.339	2	5.187E-06	8.82E-05	****	34.045	2	4.047E-08	6.88E-07	****	12.693	4	0.0129	0.2189		9.868	3	0.0197	0.3349	
12	6.305	2	0.0428	0.728777		31.69	2	1.317E-07	2.24E-06	****	1.009	1	0.3152	1		64.89	2	8E-15	1.36E-13	****	20.86	2	2.958E-05	0.0005	***	11.02	4	0.0264	0.4492		2.596	3	0.4581	1	
13	9.658	2	0.008	0.135918		8.891	2	0.0117	0.1984		5.417	1	0.0199	0.3383		71.81	2	1E-15	1.7E-14	****	8.443	2	0.0147	0.2499		37.27	4	1.58E-07	2.69E-06	****	25.18	3	1.419E-05	0.000241	***
14	3.567	2	0.1681	2.857439		10.83	2	0.0045	0.0757	*	3.011	1	0.0827	1		19.56	2	5.687E-05	0.00097	***	53.03	2	3.05E-12	5.19E-11	****	26.05	4	3.087E-05	0.0005	***	8.064	3	0.0447	0.7599	
15	16.20	2	0.0003	0.005166	**	18.38	2	0.0001	0.0017	**	0.053	1	0.8183	1		26.47	2	1.788E-06	3.04E-05	****	0.584	2	0.7468	1		13.50	4	0.0091	0.1543		11.20	3	0.0107	0.1819	
16	17.42	2	0.0001	0.002798	***	15.72	2	0.0004	0.0085	**	4.996	1	0.0254	0.4318		18.69	2	8.73E-05	0.0015	**	19.66	2	5.371E-05	0.0009	***	13.86	4	0.0078	0.1318		6.674	3	0.083	1	
17	2.801	2	0.2495	4.190361		13.47	2	0.0012	0.0204	*	1.536	1	0.2152	1		3.508	2	0.1730664	1		8.148	2	0.017	0.289		20.84	4	0.0003	0.0058	**	5.160	3	0.1604	1	

Supplemental Table 12: Characteristics of Clusters Identified based on Return Density Plots

Type	n	Mean ISI (sec)
1	689	2.8003
2	560	0.6955
3	90	1.0073
4	206	0.7236
5	48	0.6671
6	44	1.6740
7	50	3.2011
8	21	1.1290

Supplemental Table 13: Chi-Squared Tests on Trait Prevalence in Return DensityTypes

	Species			Age			Sex			State			Anesthesia			Disease			Genotype		
Type ID	Chi-square	df	P value	Adjusted P value		Chi-square	df	P value	Adjusted P value		Chi-square	df	P value	Adjusted P value		Chi-square	df	P value	Adjusted P value		Chi-square	df	P value	Adjusted P value	
1	7.886	2	0.0216	0.1728		29.36	2	4.21E-07	3.4E-06	****	11.73	1	0.0006	0.0048	**	67.24	2	3E-15	2.4E-14	****	43.13	2	4.32E-10	3.5E-09	****	77.06	4	1E-15	1.7E-14	****	7.117	3	0.0683	0.5464	
2	103.1	2	1E-15	1.7E-14	****	48.62	2	2.77E-11	2.2E-10	****	5.195	1	0.0227	0.1816		105.1	2	1E-15	1.7E-14	****	28.67	2	5.96E-07	4.8E-06	****	84.53	4	1E-15	1.7E-14	****	43.34	3	2.09E-09	1.7E-08	****
3	15.44	2	0.0004	0.0032	**	29.55	2	3.82E-07	3.1E-06	****	4.624	1	0.0315	0.252		9.159	2	0.0103	0.0824		11.34	2	0.0034	0.0272	*	32.05	4	1.87E-06	1.5E-05	****	22.90	3	4.23E-05	0.00034	***
4	91.14	2	1E-15	1.7E-14	****	79.24	2	1E-15	1.7E-14	****	9.379	1	0.0022	0.0176	*	321.8	2	1E-15	1.7E-14	****	52.02	2	5.06E-12	4E-11	****	10.31	4	0.0356	0.2848		1.395	3	0.7068	1	
5	70.36	2	1E-15	1.7E-14	****	0.039	2	0.9806	1		0.299	1	0.5848	1		101.0	2	1E-15	1.7E-14	****	0.619	2	0.7339	1		4.992	4	0.2881	1		36.01	3	7.46E-08	6E-07	****
6	4.600	2	0.1002	0.8016		1.391	2	0.4988	1		5.775	1	0.0163	0.1304		6.182	2	0.0455	0.364		19.67	2	5.35E-05	0.00043	***	7.196	4	0.1259	1		4.383	3	0.222985	1	
7	6.108	2	0.0472	0.3776		5.011	2	0.0816	0.6528		9.084	1	0.0026	0.0208	*	7.538	2	0.0231	0.1848		27.56	2	1.04E-06	8.3E-06	****	6.348	4	0.1746	1		4.891	3	0.17997	1	
8	4.533	2	0.103882	0.8295		0.668	2	0.7161	1		0.870	1	0.3509	1		25.92	2	2.35E-06	1.9E-05	****	1.778	2	0.4111	1		2.755	4	0.5996	1		24.98	3	1.56E-05	0.00012	***

References

Abercrombie ED, Jacobs BL (1987) Single-unit response of noradrenergic neurons in the locus coeruleus of freely moving cats. II. Adaptation to chronically presented stressful stimuli. J Neurosci 7:2844-2848.

Akaike T (1982) Periodic bursting activities of locus coerulleus neurons in the rat. Brain Res 239:629-633.

Almeida MC, Steiner AA, Coimbra NC, Branco LG (2004) Thermoeffector neuronal pathways in fever: a study in rats showing a new role of the locus coeruleus. J Physiol 558:283-294.

Alnaes D, Sneve MH, Espeseth T, Endestad T, van de Pavert SH, Laeng B (2014) Pupil size signals mental effort deployed during multiple object tracking and predicts brain activity in the dorsal attention network and the locus coeruleus. J Vis 14.

Altemus M, Sarvaiya N, Neill Epperson C (2014) Sex differences in anxiety and depression clinical perspectives. Front Neuroendocrinol 35:320-330.

Anderson T, Sharma S, Kelberman MA, Ware C, Guo N, Qin Z, Weinshenker D, Parent MB (2023) Obesity during preclinical Alzheimer's disease development exacerbates brain metabolic decline. J Neurochem.

Appelman Y, van Rijn BB, Ten Haaf ME, Boersma E, Peters SA (2015) Sex differences in cardiovascular risk factors and disease prevention. Atherosclerosis 241:211-218.

Aston-Jones G, Bloom FE (1981a) Activity of norepinephrine-containing locus coeruleus neurons in behaving rats anticipates fluctuations in the sleep-waking cycle. J Neurosci 1:876-886.

Aston-Jones G, Bloom FE (1981b) Norepinephrine-containing locus coeruleus neurons in behaving rats exhibit pronounced responses to non-noxious environmental stimuli. J Neurosci 1:887-900.

Aston-Jones G, Cohen JD (2005) An integrative theory of locus coeruleus-norepinephrine function: adaptive gain and optimal performance. Annu Rev Neurosci 28:403-450.

Aston-Jones G, Segal M, Bloom FE (1980) Brain aminergic axons exhibit marked variability in conduction velocity. Brain Res 195:215-222.

Aston-Jones G, Rajkowski J, Kubiak P, Alexinsky T (1994) Locus coeruleus neurons in monkey are selectively activated by attended cues in a vigilance task. J Neurosci 14:4467-4480.

Bangasser DA, Valentino RJ (2014) Sex differences in stress-related psychiatric disorders: neurobiological perspectives. Front Neuroendocrinol 35:303-319.

Bangasser DA, Wiersielis KR, Khantsis S (2016) Sex differences in the locus coeruleus-norepinephrine system and its regulation by stress. Brain Res 1641:177-188.

Bangasser DA, Zhang X, Garachh V, Hanhauser E, Valentino RJ (2011) Sexual dimorphism in locus coeruleus dendritic morphology: a structural basis for sex differences in emotional arousal. Physiol Behav 103:342-351.

Berrocoso E, Suarez-Pereira I, Llorca-Torralba M, Bravo L, Camarena-Delgado C, Soriano-Mas C (2022) The Role of the Locus Coeruleus in Pain and Associated Stress-Related Disorders. Biol Psychiat 91:786-797.

Borodovitsyna O, Flamini MD, Chandler DJ (2018) Acute Stress Persistently Alters Locus Coeruleus Function and Anxiety-like Behavior in Adolescent Rats. Neuroscience 373:7-19.

Borodovitsyna O, Tkaczynski JA, Corbett CM, Loweth JA, Chandler DJ (2022) Age- and Sex-Dependent Changes in Locus Coeruleus Physiology and Anxiety-Like Behavior Following Acute Stressor Exposure. Front Behav Neurosci 16:808590.

Bouret S, Sara SJ (2005) Network reset: a simplified overarching theory of locus coeruleus noradrenaline function. Trends Neurosci 28:574-582.

Braak H, Thal DR, Ghebremedhin E, Del Tredici K (2011) Stages of the pathologic process in Alzheimer disease: age categories from 1 to 100 years. J Neuropathol Exp Neurol 70:960-969.

Brady KT, Randall CL (1999) Gender differences in substance use disorders. Psychiatr Clin North Am 22:241-252.

Bravo L, Torres-Sanchez S, Alba-Delgado C, Mico JA, Berrocoso E (2014) Pain exacerbates chronic mild stress-induced changes in noradrenergic transmission in rats. Eur Neuropsychopharmacol 24:996-1003.

Breton-Provencher V, Sur M (2019) Active control of arousal by a locus coeruleus GABAergic circuit. Nat Neurosci 22:218-228.

Breton-Provencher V, Drummond GT, Feng J, Li Y, Sur M (2022) Spatiotemporal dynamics of noradrenaline during learned behaviour. Nature 606:732-738.

Budygin E, Grinevich V, Wang ZM, Messi ML, Meeker WR, Zhang J, Stewart WM, Milligan C, Delbono O (2024) Aging disrupts locus coeruleus-driven norepinephrine transmission in the prefrontal cortex: Implications for cognitive and motor decline. Aging Cell:e14342.

Calin-Jageman RJ, Cumming G (2019a) The New Statistics for Better Science: Ask How Much, How Uncertain, and What Else Is Known. Am Stat 73:271-280.

Calin-Jageman RJ, Cumming G (2019b) Estimation for Better Inference in Neuroscience. eNeuro 6.

Carlson JH, Foote SL (1992) Oscillation of Interspike Interval Length in Substantia-Nigra Dopamine Neurons - Effects of Nicotine and the Dopaminergic-D2 Agonist Ly-163502 on Electrophysiological Activity. Synapse 11:229-248.

Carter ME, Yizhar O, Chikahisa S, Nguyen H, Adamantidis A, Nishino S, Deisseroth K, de Lecea L (2010) Tuning arousal with optogenetic modulation of locus coeruleus neurons. Nat Neurosci 13:1526-1533.

Castelino CB, Schmidt MF (2010) What birdsong can teach us about the central noradrenergic system. J Chem Neuroanat 39:96-111.

Castren E, Thoenen H, Lindholm D (1995) Brain-derived neurotrophic factor messenger RNA is expressed in the septum, hypothalamus and in adrenergic brain stem nuclei of adult rat brain and is increased by osmotic stimulation in the paraventricular nucleus. Neuroscience 64:71-80.

Chalermpalanupap T, Schroeder JP, Rorabaugh JM, Liles LC, Lah JJ, Levey AI, Weinshenker D (2018) Locus Coeruleus Ablation Exacerbates Cognitive Deficits, Neuropathology, and Lethality in P301S Tau Transgenic Mice. J Neurosci 38:74-92.

Chandler DJ, Gao WJ, Waterhouse BD (2014) Heterogeneous organization of the locus coeruleus projections to prefrontal and motor cortices. Proc Natl Acad Sci U S A 111:6816-6821.

Chiou KL, Montague MJ, Goldman EA, Watowich MM, Sams SN, Song J, Horvath JE, Sterner KN, Ruiz-Lambides AV, Martinez MI, Higham JP, Brent LJN, Platt ML, Snyder-Mackler N (2020) Rhesus macaques as a tractable physiological model of human ageing. Philos Trans R Soc Lond B Biol Sci 375:20190612.

Cieslak PE, Llamosas N, Kos T, Ugedo L, Jastrzebska K, Torrecilla M, Rodriguez Parkitna J (2017) The role of NMDA receptor-dependent activity of noradrenergic neurons in attention, impulsivity and exploratory behaviors. Genes Brain Behav 16:812-822.

Cohen RM, Rezai-Zadeh K, Weitz TM, Rentsendorj A, Gate D, Spivak I, Bholat Y, Vasilevko V, Glabe CG, Breunig JJ, Rakic P, Davtyan H, Agadjanyan MG, Kepe V, Barrio JR, Bannykh S, Szekely CA, Pechnick RN, Town T (2013) A transgenic Alzheimer rat with plaques, tau pathology, behavioral impairment, oligomeric abeta, and frank neuronal loss. J Neurosci 33:6245-6256.

Colman RJ (2018) Non-human primates as a model for aging. Biochim Biophys Acta Mol Basis Dis 1864:2733-2741.

Conner JM, Lauterborn JC, Yan Q, Gall CM, Varon S (1997) Distribution of brain-derived neurotrophic factor (BDNF) protein and mRNA in the normal adult rat CNS: evidence for anterograde axonal transport. J Neurosci 17:2295-2313.

Coull JT (1998) Neural correlates of attention and arousal: insights from electrophysiology, functional neuroimaging and psychopharmacology. Prog Neurobiol 55:343-361.

Curtis AL, Leiser SC, Snyder K, Valentino RJ (2012) Predator stress engages corticotropin-releasing factor and opioid systems to alter the operating mode of locus coeruleus norepinephrine neurons. Neuropharmacology 62:1737-1745.

Del Negro CA, Funk GD, Feldman JL (2018) Breathing matters. Nat Rev Neurosci 19:351-367.

Delage C, Taib T, Mamma C, Lerouet D, Besson VC (2021) Traumatic Brain Injury: An Age-Dependent View of Post-Traumatic Neuroinflammation and Its Treatment. Pharmaceutics 13.

Devoto P, Flore G, Pani L, Gessa GL (2001) Evidence for co-release of noradrenaline and dopamine from noradrenergic neurons in the cerebral cortex. Mol Psychiatry 6:657-664.

Devoto P, Flore G, Saba P, Fa M, Gessa GL (2005a) Co-release of noradrenaline and dopamine in the cerebral cortex elicited by single train and repeated train stimulation of the locus coeruleus. BMC Neurosci 6:31.

Devoto P, Flore G, Saba P, Fa M, Gessa GL (2005b) Stimulation of the locus coeruleus elicits noradrenaline and dopamine release in the medial prefrontal and parietal cortex. J Neurochem 92:368-374.

Downs AM, Catavero CM, Kasten MR, McElligott ZA (2023) Tauopathy and alcohol consumption interact to alter locus coeruleus excitatory transmission and excitability in male and female mice. Alcohol 107:97-107.

Dutta S, Sengupta P (2016) Men and mice: Relating their ages. Life Sci 152:244-248.

Dvorkin R, Shea SD (2022) Precise and Pervasive Phasic Bursting in Locus Coeruleus during Maternal Behavior in Mice. J Neurosci 42:2986-2999.

Einhauser W, Stout J, Koch C, Carter O (2008) Pupil dilation reflects perceptual selection and predicts subsequent stability in perceptual rivalry. Proc Natl Acad Sci U S A 105:1704-1709.

Elman JA, Panizzon MS, Hagler DJ, Jr., Eyler LT, Granholm EL, Fennema-Notestine C, Lyons MJ, McEvoy LK, Franz CE, Dale AM, Kremen WS (2017) Task-evoked pupil dilation and BOLD variance as indicators of locus coeruleus dysfunction. Cortex 97:60-69.

Ferretti MT, Iulita MF, Cavedo E, Chiesa PA, Schumacher Dimech A, Santuccione Chadha A, Baracchi F, Girouard H, Misoch S, Giacobini E, Depypere H, Hampel H, Women's Brain P, the Alzheimer Precision Medicine I (2018) Sex differences in Alzheimer disease - the gateway to precision medicine. Nat Rev Neurol 14:457-469.

Florin-Lechner SM, Druhan JP, Aston-Jones G, Valentino RJ (1996) Enhanced norepinephrine release in prefrontal cortex with burst stimulation of the locus coeruleus. Brain Res 742:89-97.

Foote SL, Aston-Jones G, Bloom FE (1980) Impulse activity of locus coeruleus neurons in awake rats and monkeys is a function of sensory stimulation and arousal. Proc Natl Acad Sci U S A 77:3033-3037.

Fortin SM, Chen JC, Petticord MC, Ragozzino FJ, Peters JH, Hayes MR (2023) The locus coeruleus contributes to the anorectic, nausea, and autonomic physiological effects of glucagon-like peptide-1. Sci Adv 9:eadh0980.

German DC, Manaye KF, White CL, 3rd, Woodward DJ, McIntire DD, Smith WK, Kalaria RN, Mann DM (1992) Disease-specific patterns of locus coeruleus cell loss. Ann Neurol 32:667-676.

Glaser R, Kiecolt-Glaser JK (2005) Stress-induced immune dysfunction: implications for health. Nat Rev Immunol 5:243-251.

Grace AA, Bunney BS (1984) The control of firing pattern in nigral dopamine neurons: burst firing. J Neurosci 4:2877-2890.

Grant SJ, Aston-Jones G, Redmond DE, Jr. (1988) Responses of primate locus coeruleus neurons to simple and complex sensory stimuli. Brain Res Bull 21:401-410.

Grimm C, Duss SN, Privitera M, Munn BR, Karalis N, Frassle S, Wilhelm M, Patriarchi T, Razansky D, Wenderoth N, Shine JM, Bohacek J, Zerbi V (2024) Tonic and burst-like locus coeruleus stimulation distinctly shift network activity across the cortical hierarchy. Nat Neurosci.

Harley CW, Sara SJ (1992) Locus coeruleus bursts induced by glutamate trigger delayed perforant path spike amplitude potentiation in the dentate gyrus. Exp Brain Res 89:581-587.

Harley CW, Yuan Q (2021) Locus Coeruleus Optogenetic Modulation: Lessons Learned from Temporal Patterns. Brain Sci 11.

Hayat H, Regev N, Matosevich N, Sales A, Paredes-Rodriguez E, Krom AJ, Bergman L, Li Y, Lavigne M, Kremer EJ, Yizhar O, Pickering AE, Nir Y (2020) Locus coeruleus norepinephrine activity mediates sensory-evoked awakenings from sleep. Sci Adv 6:eaaz4232.

He M, Heindel WC, Nassar MR, Siefert EM, Festa EK (2020) Age-related changes in the functional integrity of the phasic alerting system: a pupillometric investigation. Neurobiol Aging 91:136-147.

Hindle JV (2010) Ageing, neurodegeneration and Parkinson's disease. Age Ageing 39:156-161.

Hirata H, Aston-Jones G (1994) A novel long-latency response of locus coeruleus neurons to noxious stimuli: mediation by peripheral C-fibers. J Neurophysiol 71:1752-1761.

Hirschberg S, Li Y, Randall A, Kremer EJ, Pickering AE (2017) Functional dichotomy in spinal- vs prefrontal-projecting locus coeruleus modules splits descending noradrenergic analgesia from ascending aversion and anxiety in rats. Elife 6.

Ho J, Tumkaya T, Aryal S, Choi H, Claridge-Chang A (2019) Moving beyond

values: data analysis with estimation graphics. Nat Methods 16:565-566.

Hou YJ, Dan XL, Babbar M, Wei Y, Hasselbalch SG, Croteau DL, Bohr VA (2019) Ageing as a risk factor for neurodegenerative disease. Nat Rev Neurol 15:565-581.

Iannitelli AF, Kelberman MA, Lustberg DJ, Korukonda A, McCann KE, Mulvey B, Segal A, Liles LC, Sloan SA, Dougherty JD, Weinshenker D (2023) The Neurotoxin DSP-4 Dysregulates the Locus Coeruleus-Norepinephrine System and Recapitulates Molecular and Behavioral Aspects of Prodromal Neurodegenerative Disease. eNeuro 10.

Joshi S, Li Y, Kalwani RM, Gold JI (2016) Relationships between Pupil Diameter and Neuronal Activity in the Locus Coeruleus, Colliculi, and Cingulate Cortex. Neuron 89:221-234.

Kalwani RM, Joshi S, Gold JI (2014) Phasic activation of individual neurons in the locus ceruleus/subceruleus complex of monkeys reflects rewarded decisions to go but not stop. J Neurosci 34:13656-13669.

Kelberman MA, Anderson CR, Chlan E, Rorabaugh JM, McCann KE, Weinshenker D (2022) Consequences of Hyperphosphorylated Tau in the Locus Coeruleus on Behavior and Cognition in a Rat Model of Alzheimer's Disease. J Alzheimers Dis 86:1037-1059.

Kelberman MA, Rorabaugh JM, Anderson CR, Marriott A, DePuy SD, Rasmussen K, McCann KE, Weiss JM, Weinshenker D (2023) Age-dependent dysregulation of locus coeruleus firing in a transgenic rat model of Alzheimer's disease. Neurobiol Aging 125:98-108.

Kelly L, Seifi M, Ma R, Mitchell SJ, Rudolph U, Viola KL, Klein WL, Lambert JJ, Swinny JD (2021) Identification of intraneuronal amyloid beta oligomers in locus coeruleus neurons of Alzheimer's patients and their potential impact on inhibitory neurotransmitter receptors and neuronal excitability. Neuropathol Appl Neurobiol 47:488-505.

Kessler RC (2003) Epidemiology of women and depression. J Affect Disord 74:5-13.

Kuo CC, Chan H, Hung WC, Chen RF, Yang HW, Min MY (2023) Carbachol increases locus coeruleus activation by targeting noradrenergic neurons, inhibitory interneurons and inhibitory synaptic transmission. Eur J Neurosci 57:32-53.

Kuo CC, Hsieh JC, Tsai HC, Kuo YS, Yau HJ, Chen CC, Chen RF, Yang HW, Min MY (2020) Inhibitory interneurons regulate phasic activity of noradrenergic neurons in the mouse locus coeruleus and functional implications. J Physiol 598:4003-4029.

Langley J, Hussain S, Huddleston DE, Bennett IJ, Hu XP (2022) Impact of Locus Coeruleus and Its Projections on Memory and Aging. Brain Connect 12:223-233.

Li L, Rana AN, Li EM, Feng J, Li Y, Bruchas MR (2023) Activity-dependent constraints on catecholamine signaling. Cell Rep 42:113566.

Li Y, Hickey L, Perrins R, Werlen E, Patel AA, Hirschberg S, Jones MW, Salinas S, Kremer EJ, Pickering AE (2016) Retrograde optogenetic characterization of the pontospinal module of the locus coeruleus with a canine adenoviral vector. Brain Res 1641:274-290.

Liu KY, Acosta-Cabronero J, Cardenas-Blanco A, Loane C, Berry AJ, Betts MJ, Kievit RA, Henson RN, Düzel E, Howard R, Hämmerer D, Cam-CAN (2020) in vivo visualization of age-related differences in the locus coeruleus (vol 74, pg 101, 2019). Neurobiology of Aging 91:172-174.

Liu Y, Rodenkirch C, Moskowitz N, Schriver B, Wang Q (2017) Dynamic Lateralization of Pupil Dilation Evoked by Locus Coeruleus Activation Results from Sympathetic, Not Parasympathetic, Contributions. Cell Rep 20:3099-3112.

Llorca-Torralba M, Pilar-Cuéllar F, Bravo L, Bruzos-Cidon C, Torrecilla M, Mico JA, Ugedo L, Garro-Martínez E, Berrocoso E (2019) Opioid Activity in the Locus Coeruleus Is Modulated by Chronic Neuropathic Pain. Mol Neurobiol 56:4135-4150.

Lovejoy JC, Sainsbury A, Stock Conference Working G (2009) Sex differences in obesity and the regulation of energy homeostasis. Obes Rev 10:154-167.

Lovett-Barron M, Andalman AS, Allen WE, Vesuna S, Kauvar I, Burns VM, Deisseroth K (2017) Ancestral Circuits for the Coordinated Modulation of Brain State. Cell 171:1411-1423 e1417.

Ludwig M, Yi YJ, Lusebrink F, Callaghan MF, Betts MJ, Yakupov R, Weiskopf N, Dolan RJ, Duzel E, Hammerer D (2024) Functional locus coeruleus imaging to investigate an ageing noradrenergic system. Commun Biol 7:777.

Ma PM (1994) Catecholaminergic systems in the zebrafish. II. Projection pathways and pattern of termination of the locus coeruleus. J Comp Neurol 344:256-269.

Manger PR, Eschenko O (2021) The Mammalian Locus Coeruleus Complex-Consistencies and Variances in Nuclear Organization. Brain Sci 11.

Mann DM, Lincoln J, Yates PO, Stamp JE, Toper S (1980) Changes in the monoamine containing neurones of the human CNS in senile dementia. Br J Psychiatry 136:533-541.

Mariscal P, Bravo L, Llorca-Torralba M, Razquin J, Miguelez C, Suarez-Pereira I, Berrocoso E (2023) Sexual differences in locus coeruleus neurons and related behavior in C57BL/6J mice. Biol Sex Differ 14:64.

Marzo A, Totah NK, Neves RM, Logothetis NK, Eschenko O (2014) Unilateral electrical stimulation of rat locus coeruleus elicits bilateral response of norepinephrine neurons and sustained activation of medial prefrontal cortex. J Neurophysiol 111:2570-2588.

Mather M, Harley CW (2016) The Locus Coeruleus: Essential for Maintaining Cognitive Function and the Aging Brain. Trends Cogn Sci 20:214-226.

Mawdsley JE, Rampton DS (2005) Psychological stress in IBD: new insights into pathogenic and therapeutic implications. Gut 54:1481-1491.

McCall JG, Al-Hasani R, Siuda ER, Hong DY, Norris AJ, Ford CP, Bruchas MR (2015) CRH Engagement of the Locus Coeruleus Noradrenergic System Mediates Stress-Induced Anxiety. Neuron 87:605-620.

McKinney A, Hu M, Hoskins A, Mohammadyar A, Naeem N, Jing J, Patel SS, Sheth BR, Jiang X (2023) Cellular composition and circuit organization of the locus coeruleus of adult mice. Elife 12.

Miguelez C, Grandoso L, Ugedo L (2011a) Locus coeruleus and dorsal raphe neuron activity and response to acute antidepressant administration in a rat model of Parkinson's disease. Int J Neuropsychopharmacol 14:187-200.

Miguelez C, Aristieta A, Cenci MA, Ugedo L (2011b) The locus coeruleus is directly implicated in L-DOPA-induced dyskinesia in parkinsonian rats: an electrophysiological and behavioural study. PLoS One 6:e24679.

Morris LS, McCall JG, Charney DS, Murrough JW (2020) The role of the locus coeruleus in the generation of pathological anxiety. Brain Neurosci Adv 4:2398212820930321.

Murphy PR, Robertson IH, Balsters JH, O'Connell R G (2011) Pupillometry and P3 index the locus coeruleus-noradrenergic arousal function in humans. Psychophysiology 48:1532-1543.

Murphy PR, O'Connell RG, O'Sullivan M, Robertson IH, Balsters JH (2014) Pupil diameter covaries with BOLD activity in human locus coeruleus. Hum Brain Mapp 35:4140-4154.

Nemeroff CB, Goldschmidt-Clermont PJ (2012) Heartache and heartbreak--the link between depression and cardiovascular disease. Nat Rev Cardiol 9:526-539.

Neves RM, van Keulen S, Yang M, Logothetis NK, Eschenko O (2018) Locus coeruleus phasic discharge is essential for stimulus-induced gamma oscillations in the prefrontal cortex. J Neurophysiol 119:904-920.

Nilsson LK, Schwieler L, Engberg G, Linderholm KR, Erhardt S (2005) Activation of noradrenergic locus coeruleus neurons by clozapine and haloperidol: involvement of glutamatergic mechanisms. Int J Neuropsychopharmacol 8:329-339.

Olpe HR, Steinmann MW (1982) Age-related decline in the activity of noradrenergic neurons of the rat locus coeruleus. Brain Res 251:174-176.

Osorio-Forero A, Cardis R, Vantomme G, Guillaume-Gentil A, Katsioudi G, Devenoges C, Fernandez LMJ, Luthi A (2021) Noradrenergic circuit control of non-REM sleep substates. Curr Biol 31:5009-5023 e5007.

Pinos H, Collado P, Rodriguez-Zafra M, Rodriguez C, Segovia S, Guillamon A (2001) The development of sex differences in the locus coeruleus of the rat. Brain Res Bull 56:73-78.

Poe GR, Foote S, Eschenko O, Johansen JP, Bouret S, Aston-Jones G, Harley CW, Manahan-Vaughan D, Weinshenker D, Valentino R, Berridge C, Chandler DJ, Waterhouse B, Sara SJ (2020) Locus coeruleus: a new look at the blue spot. Nat Rev Neurosci 21:644-659.

Poelchen W, Sieler D, Wirkner K, Illes P (2001) Co-transmitter function of ATP in central catecholaminergic neurons of the rat. Neuroscience 102:593-602.

Poller WC et al. (2022) Brain motor and fear circuits regulate leukocytes during acute stress. Nature 607:578-584.

Prokopiou PC, Engels-Dominguez N, Papp KV, Scott MR, Schultz AP, Schneider C, Farrell ME, Buckley RF, Quiroz YT, El Fakhri G, Rentz DM, Sperling RA, Johnson KA, Jacobs HIL (2022) Lower novelty-related locus coeruleus function is associated with Abeta-related cognitive decline in clinically healthy individuals. Nat Commun 13:1571.

Prouty EW, Waterhouse BD, Chandler DJ (2017) Corticotropin releasing factor dose-dependently modulates excitatory synaptic transmission in the noradrenergic nucleus locus coeruleus. Eur J Neurosci 45:712-722.

Ramirez JM, Dashevskiy T, Marlin IA, Baertsch N (2016) Microcircuits in respiratory rhythm generation: commonalities with other rhythm generating networks and evolutionary perspectives. Curr Opin Neurobiol 41:53-61.

Rorabaugh JM, Chalermpalanupap T, Botz-Zapp CA, Fu VM, Lembeck NA, Cohen RM, Weinshenker D (2017) Chemogenetic locus coeruleus activation restores reversal learning in a rat model of Alzheimer's disease. Brain 140:3023-3038.

Ross JA, Van Bockstaele EJ (2020) The Locus Coeruleus- Norepinephrine System in Stress and Arousal: Unraveling Historical, Current, and Future Perspectives. Front Psychiatry 11:601519.

Sara SJ (2009) The locus coeruleus and noradrenergic modulation of cognition. Nat Rev Neurosci 10:211-223.

Sara SJ, Bouret S (2012) Orienting and Reorienting: The Locus Coeruleus Mediates Cognition through Arousal. Neuron 76:130-141.

Saunier CF, Akaoka H, de La Chapelle B, Charlety PJ, Chergui K, Chouvet G, Buda M, Quintin L (1993) Activation of brain noradrenergic neurons during recovery from halothane anesthesia. Persistence of phasic activation after clonidine. Anesthesiology 79:1072-1082.

Schwarz LA, Luo L (2015) Organization of the locus coeruleus-norepinephrine system. Curr Biol 25:R1051-R1056.

Siegel RM (1990) Nonlinear Dynamic System-Theory and Primary Visual Cortical Processing. Physica D 42:385-395.

Simmons HA (2016) Age-Associated Pathology in Rhesus Macaques (Macaca mulatta). Vet Pathol 53:399-416.

Simpson KL, Waterhouse BD, Lin RC (1999) Origin, distribution, and morphology of galaninergic fibers in the rodent trigeminal system. J Comp Neurol 411:524-534.

Smeets WJ, Gonzalez A (2000) Catecholamine systems in the brain of vertebrates: new perspectives through a comparative approach. Brain Res Brain Res Rev 33:308-379.

Sturrock RR, Rao KA (1985a) A quantitative histological study of neuronal loss from the locus coeruleus of ageing mice. Neuropathol Appl Neurobiol 11:55-60.

Sturrock RR, Rao KA (1985b) A Quantitative Histological Study of Neuronal Loss from the Locus Coeruleus of Aging Mice. Neuropath Appl Neuro 11:55-60.

Sved AF, Felsten G (1987) Stimulation of the locus coeruleus decreases arterial pressure. Brain Res 414:119-132.

Swift KM, Gross BA, Frazer MA, Bauer DS, Clark KJD, Vazey EM, Aston-Jones G, Li Y, Pickering AE, Sara SJ, Poe GR (2018) Abnormal Locus Coeruleus Sleep Activity Alters Sleep Signatures of Memory Consolidation and Impairs Place Cell Stability and Spatial Memory. Curr Biol 28:3599-3609 e3594.

Szücs A, Abarbanel HDI, Rabinovich MI, Selverston AI (2005) Dopamine modulation of spike dynamics in bursting neurons. European Journal of Neuroscience 21:763-772.

Takeuchi T, Duszkiewicz AJ, Sonneborn A, Spooner PA, Yamasaki M, Watanabe M, Smith CC, Fernandez G, Deisseroth K, Greene RW, Morris RG (2016) Locus coeruleus and dopaminergic consolidation of everyday memory. Nature 537:357-362.

Tao Y, Li X, Dong Q, Kong L, Petersen AJ, Yan Y, Xu K, Zima S, Li Y, Schmidt DK, Ayala M, Mathivanan S, Sousa AMM, Chang Q, Zhang SC (2023) Generation of locus coeruleus norepinephrine neurons from human pluripotent stem cells. Nat Biotechnol.

Theofilas P, Ehrenberg AJ, Dunlop S, Di Lorenzo Alho AT, Nguy A, Leite REP, Rodriguez RD, Mejia MB, Suemoto CK, Ferretti-Rebustini REL, Polichiso L, Nascimento CF, Seeley WW, Nitrini R, Pasqualucci CA, Jacob Filho W, Rueb U, Neuhaus J, Heinsen H, Grinberg LT (2017) Locus coeruleus volume and cell population changes during Alzheimer's disease progression: A stereological study in human postmortem brains with potential implication for early-stage biomarker discovery. Alzheimers Dement 13:236-246.

Tkaczynski JA, Borodovitsyna O, Chandler DJ (2022) Delta Opioid Receptors and Enkephalinergic Signaling within Locus Coeruleus Promote Stress Resilience. Brain Sci 12.

Tolin DF, Foa EB (2006) Sex differences in trauma and posttraumatic stress disorder: a quantitative review of 25 years of research. Psychol Bull 132:959-992.

Totah NK, Neves RM, Panzeri S, Logothetis NK, Eschenko O (2018) The Locus Coeruleus Is a Complex and Differentiated Neuromodulatory System. Neuron 99:1055-1068 e1056.

Tovar S, Paeger L, Hess S, Morgan DA, Hausen AC, Bronneke HS, Hampel B, Ackermann PJ, Evers N, Buning H, Wunderlich FT, Rahmouni K, Kloppenburg P, Bruning JC (2013) K(ATP)-channel-

dependent regulation of catecholaminergic neurons controls BAT sympathetic nerve activity and energy homeostasis. Cell Metab 18:445-455.

Tung CS, Ugedo L, Grenhoff J, Engberg G, Svensson TH (1989) Peripheral induction of burst firing in locus coeruleus neurons by nicotine mediated via excitatory amino acids. Synapse 4:313-318.

Uematsu A, Tan BZ, Ycu EA, Cuevas JS, Koivumaa J, Junyent F, Kremer EJ, Witten IB, Deisseroth K, Johansen JP (2017) Modular organization of the brainstem noradrenaline system coordinates opposing learning states. Nat Neurosci 20:1602-1611.

van den Brink RL, Murphy PR, Nieuwenhuis S (2016a) Pupil Diameter Tracks Lapses of Attention. PLoS One 11:e0165274.

van den Brink RL, Pfeffer T, Warren CM, Murphy PR, Tona KD, van der Wee NJ, Giltay E, van Noorden MS, Rombouts SA, Donner TH, Nieuwenhuis S (2016b) Catecholaminergic Neuromodulation Shapes Intrinsic MRI Functional Connectivity in the Human Brain. J Neurosci 36:7865-7876.

van Dongen PA (1981) The human locus coeruleus in neurology and psychiatry. (Parkinson's, Lewy body, Hallervorden-Spatz, Alzheimer's and Korsakoff's disease, (pre)senile dementia, schizophrenia, affective disorders, psychosis). Prog Neurobiol 17:97-139.

Vankov A, Herve-Minvielle A, Sara SJ (1995) Response to novelty and its rapid habituation in locus coeruleus neurons of the freely exploring rat. Eur J Neurosci 7:1180-1187.

Varazzani C, San-Galli A, Gilardeau S, Bouret S (2015) Noradrenaline and dopamine neurons in the reward/effort trade-off: a direct electrophysiological comparison in behaving monkeys. J Neurosci 35:7866-7877.

Vazey EM, Aston-Jones G (2014) Designer receptor manipulations reveal a role of the locus coeruleus noradrenergic system in isoflurane general anesthesia. Proc Natl Acad Sci U S A 111:3859-3864.

Vazey EM, Moorman DE, Aston-Jones G (2018) Phasic locus coeruleus activity regulates cortical encoding of salience information. Proc Natl Acad Sci U S A 115:E9439-E9448.

Vong L, Ye C, Yang Z, Choi B, Chua S, Jr., Lowell BB (2011) Leptin action on GABAergic neurons prevents obesity and reduces inhibitory tone to POMC neurons. Neuron 71:142-154.

Vreven A, Aston-Jones G, Pickering AE, Poe GR, Waterhouse B, Totah NK (2024) In search of the locus coeruleus: guidelines to identify anatomical boundaries and physiological properties of the blue spot in mice, fish, finches and beyond. J Neurophysiol.

Wang S, Wang Z, Mu Y (2022) Locus Coeruleus in Non-Mammalian Vertebrates. Brain Sci 12.

Wang S, Lai X, Deng Y, Song Y (2020) Correlation between mouse age and human age in anti-tumor research: Significance and method establishment. Life Sci 242:117242.

Wang X, Pinol RA, Byrne P, Mendelowitz D (2014) Optogenetic stimulation of locus ceruleus neurons augments inhibitory transmission to parasympathetic cardiac vagal neurons via activation of brainstem alpha1 and beta1 receptors. J Neurosci 34:6182-6189.

Weinshenker D (2018) Long Road to Ruin: Noradrenergic Dysfunction in Neurodegenerative Disease. Trends Neurosci 41:211-223.

Weinshenker D, Schroeder JP (2007) There and back again: a tale of norepinephrine and drug addiction. Neuropsychopharmacology 32:1433-1451.

Whitacre CC (2001) Sex differences in autoimmune disease. Nat Immunol 2:777-780.

Williams PA, Rahmouni K (2022) Crosstalk in the Central Autonomic Neurocircuitry Underlying Cardiovascular and Metabolic Control. Faseb J 36.

Witten IB, Steinberg EE, Lee SY, Davidson TJ, Zalocusky KA, Brodsky M, Yizhar O, Cho SL, Gong S, Ramakrishnan C, Stuber GD, Tye KM, Janak PH, Deisseroth K (2011) Recombinase-driver rat lines: tools, techniques, and optogenetic application to dopamine-mediated reinforcement. Neuron 72:721-733.

Yang B, Sanches-Padilla J, Kondapalli J, Morison SL, Delpire E, Awatramani R, Surmeier DJ (2021) Locus coeruleus anchors a trisynaptic circuit controlling fear-induced suppression of feeding. Neuron 109:823-838 e826.

Zaib S, Javed H, Khan I, Jaber F, Sohail A, Zaib Z, Mehboob T, Tabassam N, Ogaly HA (2023) Neurodegenerative Diseases: Their Onset, Epidemiology, Causes and Treatment. Chemistryselect 8.

Zhang S, Hu SE, Chao HH, Li CSR (2016) Resting-State Functional Connectivity of the Locus Coeruleus in Humans: In Comparison with the Ventral Tegmental Area/Substantia Nigra Pars Compacta and the Effects of Age. Cereb Cortex 26:3413-3427.

Ziegler DR, Cass WA, Herman JP (1999) Excitatory influence of the locus coeruleus in hypothalamic-pituitary-adrenocortical axis responses to stress. J Neuroendocrinol 11:361-369.

Disclosures and Conflicts of Interest

Qi Wang and Charles Rodenkirch are the founders of Sharper Sense, a company developing methods of enhancing sensory processing with neural interfaces. Alfred P. Kaye receives or has received research funding from Transcend Therapeutics and Freedom Biosciences, and has filed a provisional patent for combination psychedelic pharmacotherapies in PTSD. Anthony E Pickering reports research funding from Eli Lilly and is a member of the advisory board for Lateral Pharma. All other authors report no disclosures or conflicts of interest. Nelson K. Totah has filed a provisional patent for a head-fixation attachment for the skull of a rat and method for installing the attachment.

CRediT authorship contribution statement

Conceptualization: Nelson K. Totah

Data Curation: Michael A. Kelberman, Ellen Rodberg, Liping Zhao

Formal Analysis: Michael A. Kelberman, Ellen Rodberg, Liping Zhao

Investigation: Vincent Breton-Provencher, Chloe J. Bair-Marshall, Daniel J. Chandler, Chih-Cheng Chen, Ruei-Feng Chen, Oscar Davy, David M. Devilbiss, Anthony M. Downs, Gabrielle Drummond, Roman Dvorkin, Zeinab Fazlali, Erin Glennon, Jung-Chien Hsieh, Hiroki Ito, Michael A. Kelberman, Jenny R. Kim, Chao-Cheng Kuo, Yu-Shan Kuo, Rong-Jian Liu, Yang Liu, Meritxell Llorca-Torralba, Andrew M. McKinney, Alexandra C. Nowlan, Yadollah Ranjbar-Slamloo, Jone Razquin, Ellen Rodberg, Charles Rodenkirch, Anna C. Sales, Rath Satyasambit, Stephen D. Shea, Hsing-Chun Tasi, John Arthur Tkaczynski, Sonia Torres-Sanchez, Akira Uematsu, Chayla R. Vazquez, Amelien Vreven, Hsiu-Wen Yang, Jen-Hau Yang, Hau-Jie Yau, Liping Zhao, Ioannis S. Zouridis

Methodology: Michael A. Kelberman, Nelson K. Totah, Ellen Rodberg, Liping Zhao

Project Administration: Nelson K. Totah, Elena Vazey, David Weinshenker

Resources: Ehsan Arabzadeh, Esther Berrocoso, David M. Devilbiss, Robert C. Froemke, Joshua I. Gold, Xiaolong Jiang, Joshua P. Johansen, Alfred P. Kaye, Jordan G. McCall, Zoe A. McElligott, Cristina Miguelez, Ming-Yuan Min, Anthony E. Pickering, Stephen D. Shea, Mriganka Sur, Nelson K. Totah, Elena M Vazey, Qi Wang, David Weinshenker

Software: Michael A. Kelberman, Nelson K. Totah, Ellen Rodberg, Liping Zhao

Supervision: Nelson K. Totah, Elena Vazey, David Weinshenker

Validation: Michael A. Kelberman, Nelson K. Totah, Ellen Rodberg, Liping Zhao

Visualization: Michael A. Kelberman, Nelson K. Totah, Ellen Rodberg

Writing – Original Draft: Michael A. Kelberman, Nelson K. Totah, Ellen Rodberg

Writing – Review and Editing: Elena Vazey, David Weinshenker, Gina R. Poe, Barry D. Waterhouse

Funding

This work was supported by funding afforded to the following people:

- Chloe J. Bair-Marshall – Natural Sciences and Engineering Research Council of Canada PGS-D Fellowship
- Craig W. Berridge and David M. Devilbiss – NIH DA10981 and MH14602

- Esther Berrocoso – Grant No. PID2022-142785OB-I00 funded by Ministerio de Ciencia, Innovación y Universidades (MICIU)/Agencia Estatal de Investigacion (AEI)/10.13039/501100011033 and " ERDF A way of making Europe, " by the European Union ", Grant No. PDC2022-133987-100 funded by MICIU/AEI/10.13039/501100011033 and " European Union NextGenerationEU/PRTR", Red Española de Investigación en Estrés/Spanish Network for Stress Research RED2022-134191-T financed by MICIU/AEI/10.13039/501100011033, and the "CIBERSAM": CIBER -Consorcio Centro de Investigación Biomédica en Red CB07/09/0033
- Vincent Breton-Provencher – Young Investigator Award from Brain & Behavior Research Foundation, Future Leaders in Canadian Brain Research Program from Brain Canada, Natural Sciences and Engineering Research Council of Canada Discovery Grant RGPIN-2021-03284, New Frontiers in Research Fund NFRFE-2022-00342, and Research Scholars Junior 1 Salary Award from Fonds de recherche du Québec Santé 311492
- Daniel J. Chandler - NIH R56-MH121918 and R21-DA058215
- Oscar Davy and Anna Sales – Wellcome Trust PhD Programme in Neural Dynamics ref. 108899/Z/15
- Anthony Downs – T32-AA007573
- Gabrielle Drummond – NIH F31-MH129112-01A1
- Roman Dvorkin – National Alliance for Research on Schizophrenia and Depression Young Investigator Grant from the Brain and Behavior Research Foundation
- Robert C. Froemke – NIH R01-DC012557 and NIH Brain Initiative U19-NS107616
- Erin Glennon – NIDCD Predoctoral Fellowship F30-DC017351
- Joshua I. Gould – NIH R21-MH093904
- Xiaolong Jiang – NIH R01-NS101596, NIH R01-MH109556, and T32-EY07001
- Joshua P. Johansen – KAKENHI 21H00219
- Alfred P. Kaye – Brain & Behavior Research Foundation NARSAD Young Investigator Award, NIH K08MH122733, NIH R21MH134183, VA National Center for PTSD, and CT Department of Mental Health and Addiction Services
- Michael A. Kelberman – NIH F31-AG069502 and T32-MS96050
- Jordan G. McCall – NIH R01-NS117899
- Zoe A. McElligott – NIH U01-AA020911-0851, R01-DA049261, and UNC Dissertation Completion Fellowship
- Cristina Miguelez - PID2 021-126434OB-I00 funded by MCIN/AEI/10. 13039/501100011033 and ERDF A way of making Europe, Basque Government (IT1706-22) and Transborder Joint Laboratory (LTC) "non-motor Comorbidities in Parkinson's Disease (CoMorPD)"Ming-Yuan Min - Minister of Science and Technology Taiwan Grant Number: 105-2320-B-002-055-MY3
- Mohsen Omrani – CIHR Banting PDF BPF-151096
- Anthony E Pickering – Wellcome Trust Senior Clinical Fellowship gr088373 and NIH R01 DK098361
- Gina R. Poe – NIH R01-MH600670
- Ellen M. Rodberg – NIH F31-MH131348
- Stephen D. Shea – NIH R01-MH119250
- Mriganka Sur – NIH R01-MH126351, R01-MH133066, and R01-MH085802, and the Simons Foundation Autism Research Initiative through the Simons Center for the Social Brain
- Nelson K. Totah – Research Council of Finland PROFI6 funding program (UHBRAIN project), start-up funding from the Helsinki Institute of Life Science at the University of Helsinki, and National Institutes of Health BRAIN Initiative Grant 1R34NS123876.
- Akira Uematsu – JPMJFR2243, AMED-PRIME, KAKENHI 21H05176 and 22H02942

- Chayla R. Vazquez – NSF GRFP DGE-2139839
- Qi Wang – NIH R01-MH112267, R01-NS119813, and R21-MH125107
- Barry D. Waterhouse – NSF IOS-2128543
- Elena M Vazey – NIH U01-AA025481, R00-MH104716
- David Weinshenker – NIH R01-AG062581, RF1-AG079199, and RF1-AG061175
- Hsiu-Wen Yang - Minister of Science and Technology Taiwan Grant Number: 103-2302-B040-010-MY3